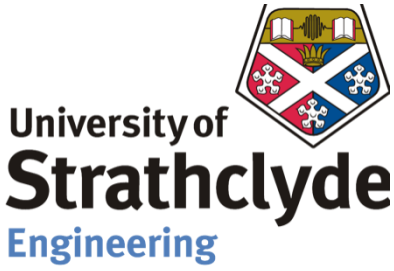

DEPARTMENT OF MECHANICAL & AEROSPACE ENGINEERING

Modelling of concentrated solar power systems to supply power to the mining sector - a case study in Zambia

Author: **Noah Masuzyo Panda**

Supervisor: **Dr Ioannis Kokkinakis**

A thesis submitted in partial fulfilment for the requirement of degree in

Master of Science in *Sustainable Engineering: Renewable Energy and the Environment*

2021

Copyright Declaration

Signed: M.N. Panda Date:17/08/2021

Acknowledgements

First and foremost, I would like to thank God, the creator of heaven and earth for the gift of life and the opportunity of staying and successfully completing a master's degree in the United Kingdom. I wish to express utmost gratitude to University of Strathclyde and Commonwealth Scholarship Commission (CSC) for fully funding my master's course. Without their financial support I could not have had the chance to study at one of Scotland's top higher learning institutions, University of Strathclyde.

I also wish to appreciate my mum, brother, sister and fiancée for the love, help and support they gave me during my tenure at Strathclyde. Lastly, I would love to give special recognition to my supervisor, Dr Ioannis Kokkinakis, for the help and support he gave me during the course of the project. This project would not have been completed successfully without the time he set aside from his busy schedule to help me.

Abstract

Zambia's economy is greatly dependent on mining. Copper exports contribute nearly 70% of the country's foreign export earnings. Zambia produces nearly 20% of the world's emeralds. There is a significant level of mining activity in the country which translates to huge electrical energy input. Mining activity accounts for approximately 50% of total electricity consumed in the country. The case study site used in this work is Chambishi Copper Smelter which is in Copperbelt province of Zambia. The annual energy consumption of the smelter for 2020 was 134.526GWh. This energy could have been enough to provide power for 36000 homes for one year in the country where the rural access to electricity stands at a meager 4% while that for urban areas stands at 67%. Thus, finding clean and sustainable solutions for Zambia's mining industry is a major step towards ensuring access to clean, reliable, sustainable and modern energy for all in line with Sustainable Development Goal number 7 of the United Nations.

In this work System Advisor Model (SAM) software is used to simulate performance of 50MW Parabolic Trough Collector (PTR) Concentrated Solar Power (CSP), 50MW Linear Fresnel Receiver (LFR) CSP and 50MW Solar Tower (ST) CSP for integration at the copper smelter plant. SAM makes performance predictions and cost of energy estimations for power projects based on weather data, system design parameters, installation and operating costs that are specified as inputs to the models. To validate results, a real life existing CSP plant in Spain, 49.9MW Andasol 3, is modelled and the results compared to actual performance of the plant.

Results revealed that Solar Tower CSP had the highest output of 174.98GWh. Solar Tower CSP produced 32.6% more electricity than parabolic trough and 33.4% more than linear Fresnel CSP. Furthermore, solar tower CSP had the highest capacity factor of 44.4% which implied that it made use of 44.4% of its rated available output capacity for the analysis year resulting in savings in excess of $12.64M annually. The Levelized Cost of Electricity (LCOE) of the solar tower CSP was higher than that of the LFR and PTC systems. Non the less, the reported value was nearly 5 cents lower than the global average LCOE for concentrated solar power which stood at 18.2 cents/KWh as of 2020 (Pitz-Paal *et al*., 2020).

The findings of this work suggest that Solar Tower CSP is the most suitable choice for the case study site. The development of a 50MW gross power output Solar Tower CSP plant was found to be practically and financially feasible. The net capital cost of this model was $350.074M. At an internal rate of return of 11.0%, the investment would be recovered after 20years of operation.

Table of Contents

List of figures

List of Tables

Acronyms

CSP	Concentrated Solar Power
C	Dollar Cents
DNI	Direct Normal Irradiation
CAPEX	Capital Expenditure
GHI	Global Horizontal Irradiation
GW	Giga Watt
h	Hour
HTF	Heat Transfer Fluid
IEA	International Energy Agency
IRENA	International Renewable Energy Agency
KW	Kilo Watt
LCOE	Levelized Cost of Electricity
LFR	Linear Fresnel Receiver
MW	Mega Watt
NPV	Net present value
NREL	National Renewable Energy Laboratory
PTC	Parabolic Trough Receiver
SAM	System Advisor Model
SDGs	Sustainable Development Goals
ST	Solar Tower
SM	Solar Multiple
TES	Thermal Energy Storage
TMY	Typical Meteorological Year
ZESCO	Zambia Electricity Supply Corporation
$	United States Dollar

1 Introduction

1.1 Background

Zambia, a landlocked country in southern central Africa, is a country endowed with a great solar and hydropower potential. Despite recent economic growth actualisation to lower middle-income class, there is a growing power crisis. The average household connected to the national power grid experiences several hours without power daily. This has drastically affected local small businesses that depend on electricity to operate. The total installed electricity generation capacity was 2981MW as of December 2019. 80.45% of this is hydro based and less than 3% is generated from renewable energy sources as depicted in the pie chart in Figure 1. Electricity produced from coal, Heavy Fuel Oil (HFO), and diesel account for approximately 16.56% of total installed capacity. The current electricity supply deficit stands at 425MW (Energy Regulation Board, 2019).

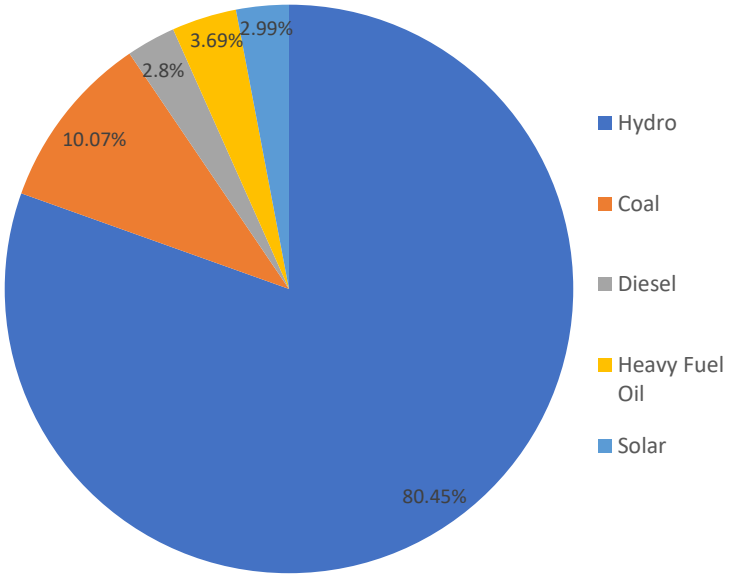

Figure 1 Installed Capacity by Technology 2019

Zambia's economy is tremendously dependent on mining. Copper export alone contributes nearly 70% towards the country's foreign export earnings. Zambia also produces roughly 20% of the world's emeralds. There is a significant level of mining activity in the country which translates to huge electrical energy input. Mining activity accounts for approximately 50% of total electricity consumed in the country. Other countries whose economy also rely heavily on mining compare poorly to Zambia's statistics. In Chile and Australia, mining only accounts for around 20% and 9% of the total energy consumed respectively (Mining for Zambia, 2016). As a consequence of this, the population access to electricity in Zambia is 31%. The rural access to electricity stands at a meager 4% while that for urban areas stands at 67% with the average household consumption of 312kWh (United States Agency for International Development (USAID), 2020).

1.1.1 Statement of purpose

Sustainable Development Goal (SDG) number 7 of the United Nations aims to achieve 100% global access to electricity. To achieve this target, considering population growth as well as disruptions arising from the COVID-19 pandemic, a target of 940 million people must gain access to electricity by the year 2030. The latest report from International Energy Agency (IEA) revealed that CO_2 emissions from electricity generation are projected to increase by 3.5% in 2020 and 2.5% in 2022. Projections from EIA further revealed that fossil fuel-based electricity will cover up to 40% of additional electricity demand in 2022. In order to achieve net-zero emissions by 2050, electricity generation emissions from coal have to decline by more than 6% a year (IEA, 2021).

In order to achieve the goals highlighted, countries with great solar energy potential need to utilize their resource. The new dawn for African countries and for many developing countries with good solar energy resource is solar energy technologies. Concentrated Solar Power (CSP) technology is one of the few viable clean energy technologies that have the potential to help decarbonize developing countries that have good solar resource. The most notable advantage of CSP technology is that it can be coupled with Thermal Energy storage (TES). TES allows the generation of electricity to be shifted to times of high demand or times of no sunlight at all. (Craig, Brent and Dinter, 2017).

The area of concentrated solar power is one that has barely been explored in Zambia. Solar photovoltaic makes up much of the 2.99% contributed by solar energy resources to the total installed capacity in the country. This work takes particular interest in accessing the feasibility of Concentrated Solar Power (CSP) systems. Research by Mwanza *et al.*, 2017 revealed that Zambia has a solar potential of 20,442TWh/year and receives on average 2109.97kWh/m^2 of solar irradiance energy per year with 4403.12 sunshine hours. There is need to make use of this solar potential for Zambia to effectively contribute towards improvement of access to electricity as well as lowering carbon emissions. It is vital that Zambia contributes towards SDG number 7 of the United Nations sustainably.

1.2 Aim

The aim of this project was to model and assess the feasibility of providing power for a copper smelter plant with electrical energy produced from concentrated solar energy. Thereafter, analyze to what extent the modeled plants meet that electrical load requirement of the case study site.

1.3 Objectives

The objectives of this project were to:

1. Understand the operation of CSP plants through literature review.
2. Assess the weather profile at the case study site for suitability to host a CSP plant.
3. Model and Simulate Solar Tower (ST) CSP, Parabolic Trough Collector (PTC) CSP and Linear Fresnel Receiver (LFR) CSP systems to review suitability based on performance and financial metrics.

1.4 Scope

The project was limited to the modelling and performance simulation of Solar Tower Parabolic Trough Collector and Linear Fresnel Receiver CSP systems. Consideration of key inputs such as net output, solar multiple, Design Point Direct Normal Irradiation (DNI) and thermal storage hours shall be optimized to provide highest level of performance. Solar Dish CSP systems are not covered in the simulations as they are not commercially deployed. Nonetheless, they are covered in literature review.

1.5 Resources

The key software used in this project was System Adviser Model (SAM). SAM is a software tool that was developed by National Renewable Energy Laboratory (NREL) with financial support from the United States Department of Energy (DOE). It is available for free and may be used for commercial, educational or personal purposes. The weather resource files used in this analysis were downloaded from National Solar Radiation Database (NRSDB) of the United States of America. NRSBD is an online database of weather files containing solar resource data in the SAM csv format. Other resources used include Excel, Publisher and MS Project.

1.6 Case study site

The case study site used in this project is Chambishi Copper Smelter plant located in Chambishi, Zambia. The plant has an annual production capacity of 250,000tons of blister copper and anodes, 5000tons of recovered copper concentrate and 380,000litres of sulphuric acid. The annual energy consumption at the smelter plant for 2020 was 134.526GWh according to daily electricity energy consumption figures availed to this project by the company. This energy could have been enough to provide power for nearly 36,000 homes for one year in the country.

2.0 Literature Review

2.1 State of Concentrated Solar Power Technology

Concentrated Solar Power (CSP) technology goes back as far as 1870 when the United States of America first designed and tested an experimental solar trough system. France followed the trend and build a Linear Fresnel pilot project in 1926. Concentrated solar technology has seen significant growth since then boasting as a viable modern day technology with potential to contribute towards provision of clean power and reducing electrical energy deficit in many countries across the world (Py, Azoumah and Olives, 2013). CSP systems have been installed in 23 countries across the world as of the year 2020 (see Figure 2).

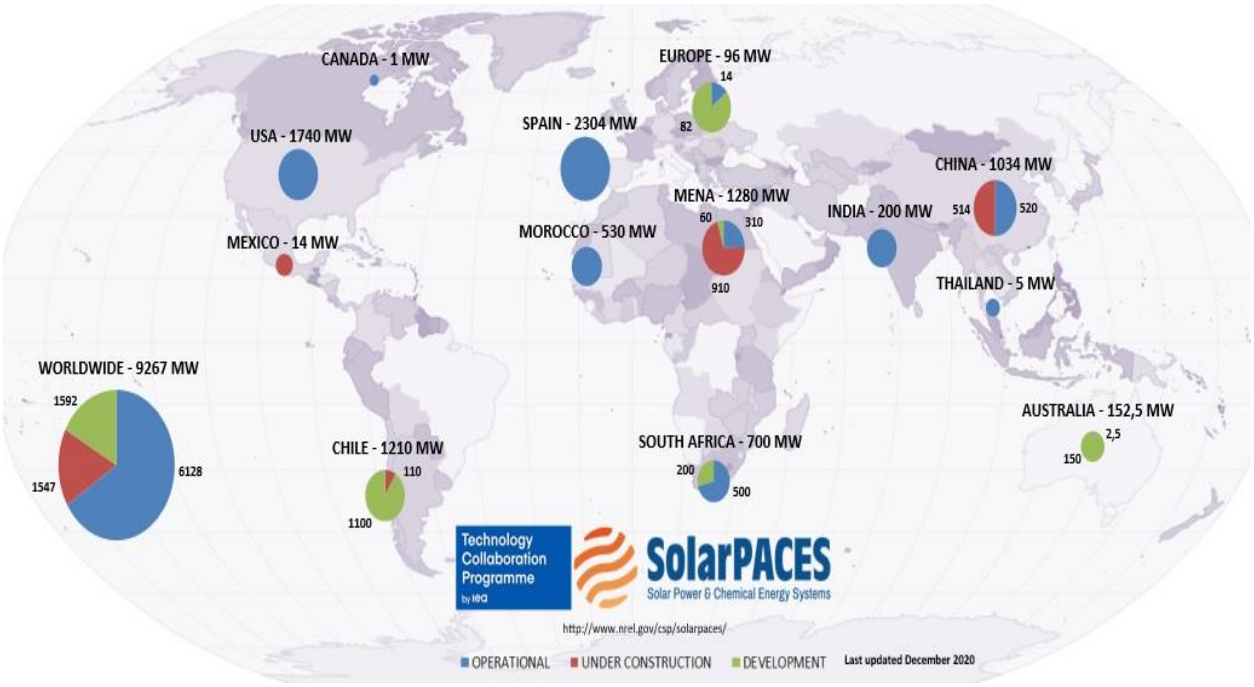

Figure 2 CSP Projects around the world (SolarPACES, 2020)

According to the International Energy Agency (IEA), in 2019 600MW (20% decrease compared to 2018 figures) of CSP capacity was added to total installed capacity across the world. According to the agency, major development was led by Israel which added 230MW. China was second with 200MW and South Africa coming in third at a 100MW while Kuwait saw the commission of a 50MW CSP plant. IEA projections indicate that growth in CSP installed capacity is expected to climb especially in emerging economy countries such as Morocco and South Africa with good solar resource (Bojek, 2020). As an emerging technology, CSP is on a trajectory of growth.

2.2 Application of Renewable Energy Power Systems in Mining Industry

Mining is one of the highest energy consuming sectors in the world today. Despite being a major source of raw material for many products across the world, the rising mineral demand and falling ore grade is likely to increase the energy demand of the sector. In the past decade there has been notable growth of renewable energy incorporation in the mining industry. Renewable energy plant installation has grown from almost being nonexistent before the year 2000 to having an annual installation of more than 3000MW in 2019. Figure 3 elaborates more on the growth of renewable energy projects in the mining sector across the world. Wind, mini or small hydro, solar and geothermal are among the leading the renewable energy technologies being incorporated by mines in day-to-day operations.

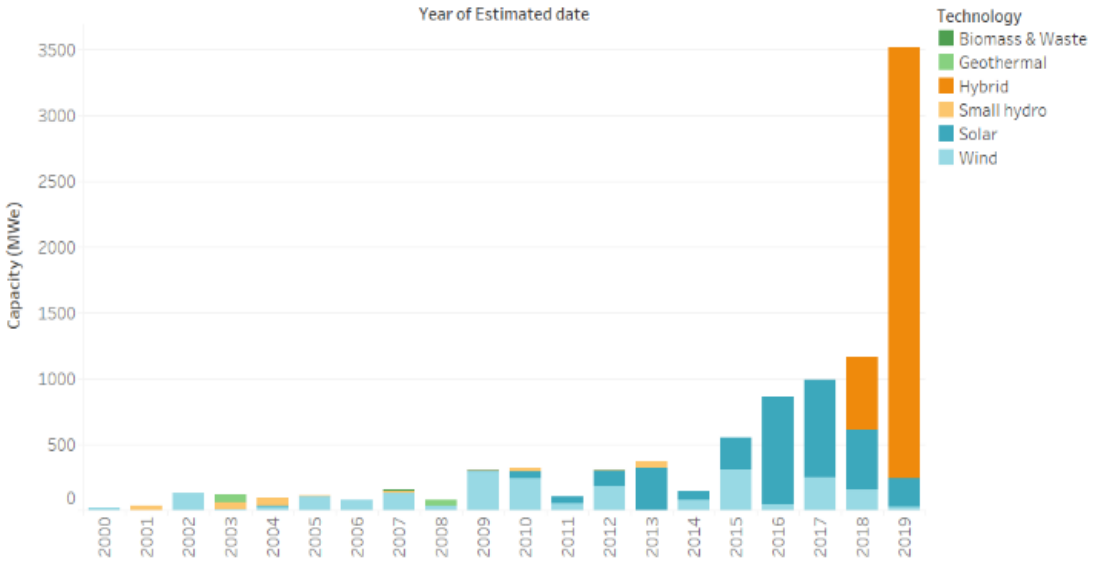

Figure 3 Renewable projects associated with mining companies worldwide (Bloomberg New Energy Finance 2019)

Majority of systems adopted in the mines are mostly hybrid systems boasting a combination of wind, solar and energy storage alongside fossil fuel backup. This is so because of the relatively high intermittence, particularly with wind and photovoltaic systems. CSP technologies with thermal energy storage which have less intermittence are now being exploited for feasibility to provide part of the power used in mining. It should be realized that 15%- 40% of total operating costs in mining is dedicated to energy import and production (Igogo *et al.*, 2020).

A recent CSP project launched to provide power to a mining sector is in Chile, South America. The Copiapó Solar Energy Project, located in the Atacama Desert in northern Chile, will generate 1,800 gigawatt hours (GWh) annually once in operation. The CSP system will have 14 hours of full-load storage, thus allowing it to produce up to 260 MW of 24/7 firm baseload power which is critical to the mining sector (Link, 2021).

2.3 Concentrated Solar Power Technologies

2.3.1 A Brief Operational Overview

The operation of CSP systems is based on the same principle. All CSP systems convert solar energy into thermal energy using solar concentrating techniques. The solar energy from the sun is reflected onto solar energy receivers by optical concentrators. A solar collector is a heat exchanging device that converts solar radiation into thermal energy. Thermal energy captured is carried away by a Heat Transfer Fluid (HTF) which is typically a molten salt, steam or synthetic oil with high heat capacity. The chemistry of the fluid varies with the technique of capture employed by the CSP system. The HTF is the life blood of power generation in CSP systems. The thermal energy it carries is used to produce steam that is in turn used to drive a steam turbine coupled to a generator. Figure 4 shows a meek overview of the of a basic principle of operation of CSP systems.

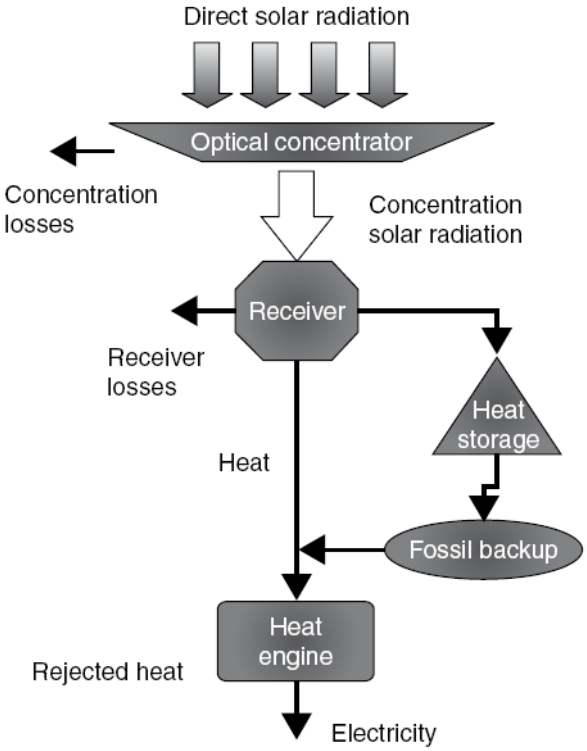

Figure 4: Basic principle of operation in CSP technology

CSP systems are classified into two major categories: point focusing and line focusing systems. Line focusing systems concentrate solar energy from the sun onto linear absorber tubes through which HTF flows. The reflectors in line focusing systems rotate about a single axis to track the location of the sun and reflect its irradiation onto the linear receiver. These systems usually have an operating temperature of 350 ^{o}C to 550^{o}C. Point focusing systems use reflectors that concentrate the solar radiation onto a single point called a focal point. At the focal point is a central receiver that harnesses the energy in the concentrated sunlight. Figure 5 shows the classification of CSP systems.

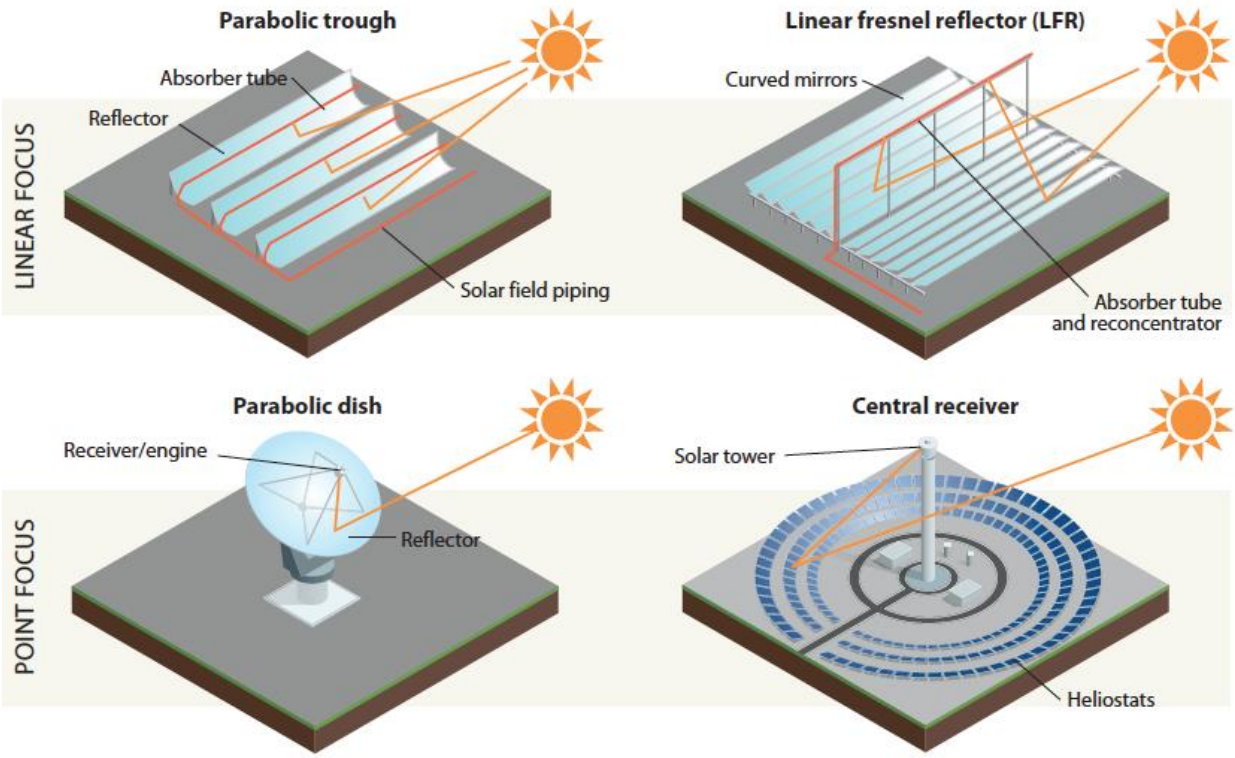

Figure 5 Classification of CSP systems

2.3.2 Parabolic Trough Collector CSP

A Parabolic Trough Collector (PTC) gets its name from the unique parabolic shaped mirrors that are used. In a PTC system parabolic tough mirror are used to concentrate sunlight onto tubular receivers. These receivers are fixed lengthwise along the focal point of the trough mirrors. Through the receiver runs thermal fluid which is the very life blood of any CSP system. The thermal fluid can either be synthetic oil or nitrate salt. The thermal fluid captures the concentrated solar energy as thermal energy. The thermal energy is used to produce steam that in turn drives a steam turbine generator. The system might also make use of a thermal energy storage system that can allow it to store energy in the form of thermal energy to be utilized later when the sun is not shining or when need arises. A basic schematic of PTC system is shown in Figure 6.

Most trough systems in operation today use high temperature synthetic oil as the HTF. The temperature limit of the oil is 400 ^{0}C. The oil becomes unstable at higher temperatures of operation which results in production of hydrogen gas. The gas, if not separated from the oil, reduces the heat transfer effectiveness of the oil. This high temperature sensitivity of oil requires that system utilizing synthetic oil are regularly maintained to ensure optimal plant operation (Heller, 2017).

The solar collectors in PTC systems are shaped like parabolas. The placement of these mirrors is symmetrical about the axis of rotation. The tracking of the suns position across

the sky enables the mirrors to ensure a greater portion of solar radiation incident on them is concentrated on the solar receivers fixed on the parabolic line of focus.

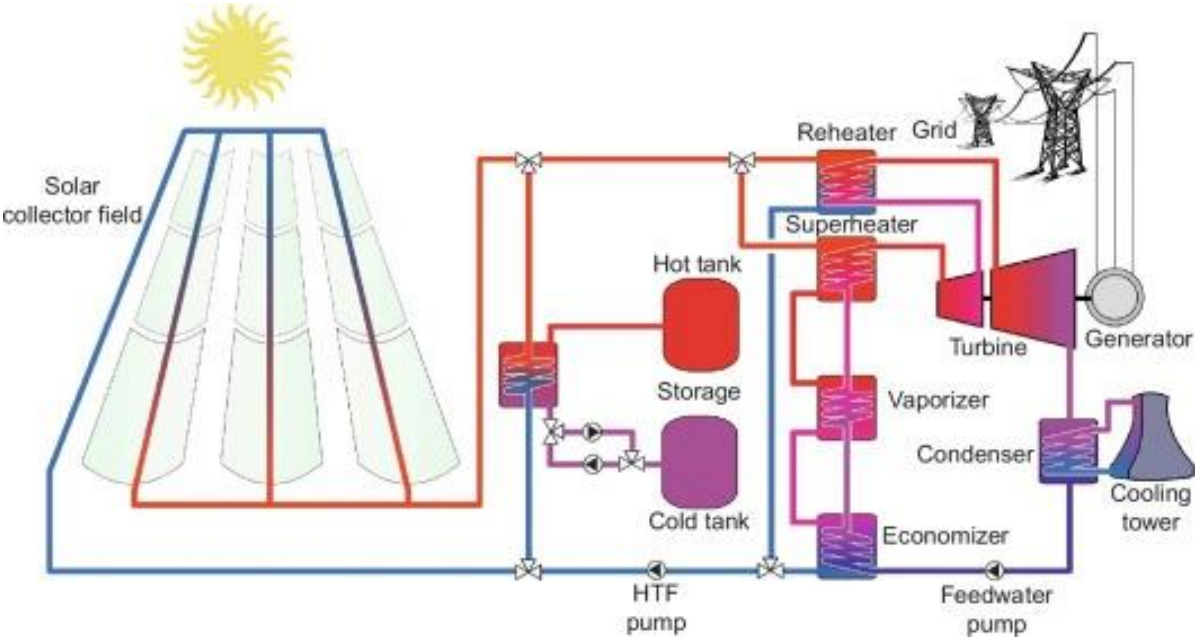

Figure 6 basic schematic of parabolic trough system (Heller, 2017)

Figure 7 La Africana parabolic trough CSP plant in Spain (source: https://www.energy.sener/projects/la-africana-parabolic-trough-plant-50mwe)

Figure 7 shows La Africana parabolic trough CSP plant, a 50MW parabolic trough solar power plant in Spain which has been operational since 2012. Other eminent PTC installations are found in South Africa. These are Bokpoort (50MW), Ilanga 1(100MW), Kathu Solar Park (100MW), KaXu Solar One (100MW) and Xina Solar One (100MW).

The PTC solar power systems are the most deployed amongst the four types of CSP systems (SolarPACES, 2020).

2.3.3 Linear Fresnel Reflector CSP

Linear Fresnel Reflector (LFR) CSP systems uses a series of flat (or slightly parabolic) shaped mirrors that reflect light onto a central receiver that is fixed on top of the collection of the mirrors. The mirrors are arranged in a manner such that the shape they form resembles that of a parabola. The long flat reflectors are called Fresnel mirrors because they bear resemblance to a Fresnel lens. The unique arrangement of the mirrors produces a concentrating effect like that of a mirror with a large aperture area and short focal length. The basic principle of operation of LFR CSP systems is shown in Figure 8.

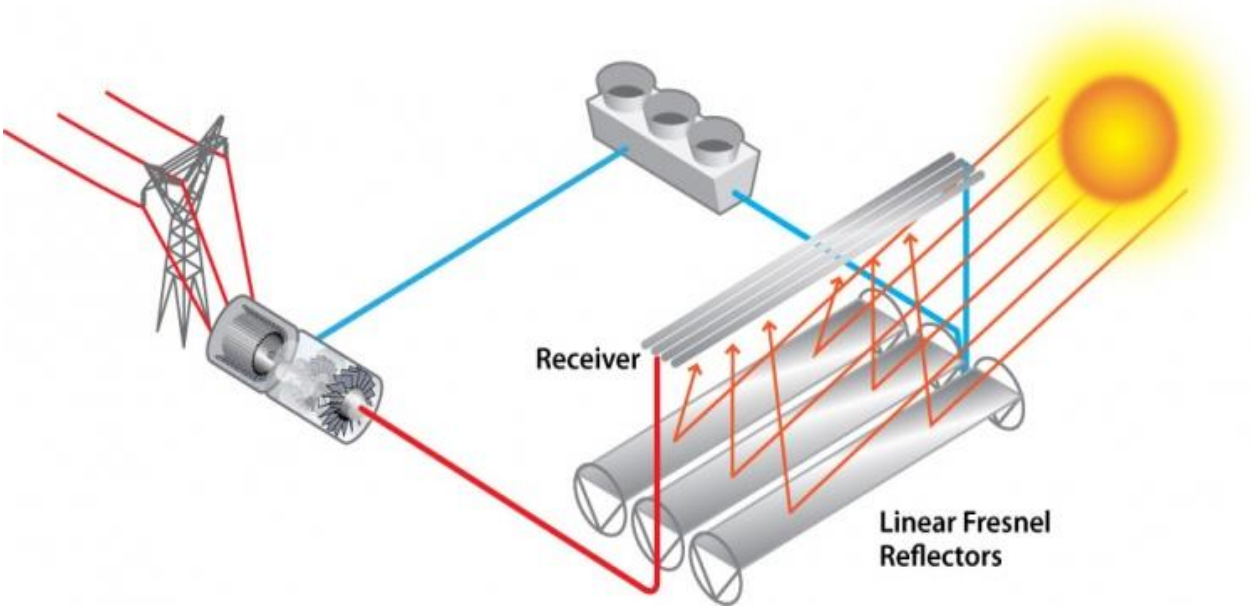

Figure 8 Basic layout of LFR CSP system

The principle of operation in these systems is the same as that employed in PTC system. However, the working fluid used in LFR systems is usually steam. LFR systems have some significant advantage over PTC systems. The reflectors used are usually flat or slightly curved to make the manufacturing process less expensive. Additionally, only the Fresnel mirrors track the sun in these systems while the central collector remains stationary unlike the situation with PTC systems where both the mirrors and the collector move relative to the sun. The support structure in these systems is also simpler and cheaper. This is attributed to the fact that reflectors are mounted close to the ground and that material is saved by not attaching the collector to the mirrors (Alinta Energy, 2014).

The most recent commission of a LFR CSP system was in China. The Duncheng 50MW molten salt Fresnel system has 13 hours of molten salt storage backup and operates on a Rankine steam power cycle. Other installations are found in several countries across the world. Although LFR systems not so common, the technology is promising. (SolarPACES, 2020)

2.3.4 Solar Tower Receiver CSP

Solar tower or central receiver CSP system uses thousands of mirrors which reflect and concentrate sunlight onto a central point at the top of a tower which in turn is used to generate electricity. These specially engineered tracking mirrors called heliostats are spread on a huge plain area which can be several square kilometres in area. The heliostats reflect and concentrate sunlight onto a large heat exchanger called a receiver that sits on top of a tower. Inside the receiver flows a HTF which can be nitrate salt or high temperature synthetic oil. The HTF absorbs the heat from the concentrated sunlight and carries it away for steam production.

The steam produced is then used to drive steam turbine generators to produce electricity. Once the hot HTF is used to produce steam the cool molten salt is in a storage tank at a lower temperature before it is allowed to flow back up to the solar energy receiver to be heated. After the steam is created, it is used to drive a steam turbine. After passing through the turbine, it is condensed back to water and returned to the water holding tank where it will flow back into the steam generator when needed. The steam produced in solar tower CSP must have a high quality super-heated steam having enough pressure to drive a standard steam turbine at maximum efficiency. This ensures the electricity generated is both reliable and non-intermittent. This technology is one hundred percent renewable remitting no greenhouse gas to the environment. Power plants employing this technology can provide on demand reliable clean electricity when coupled with TES.

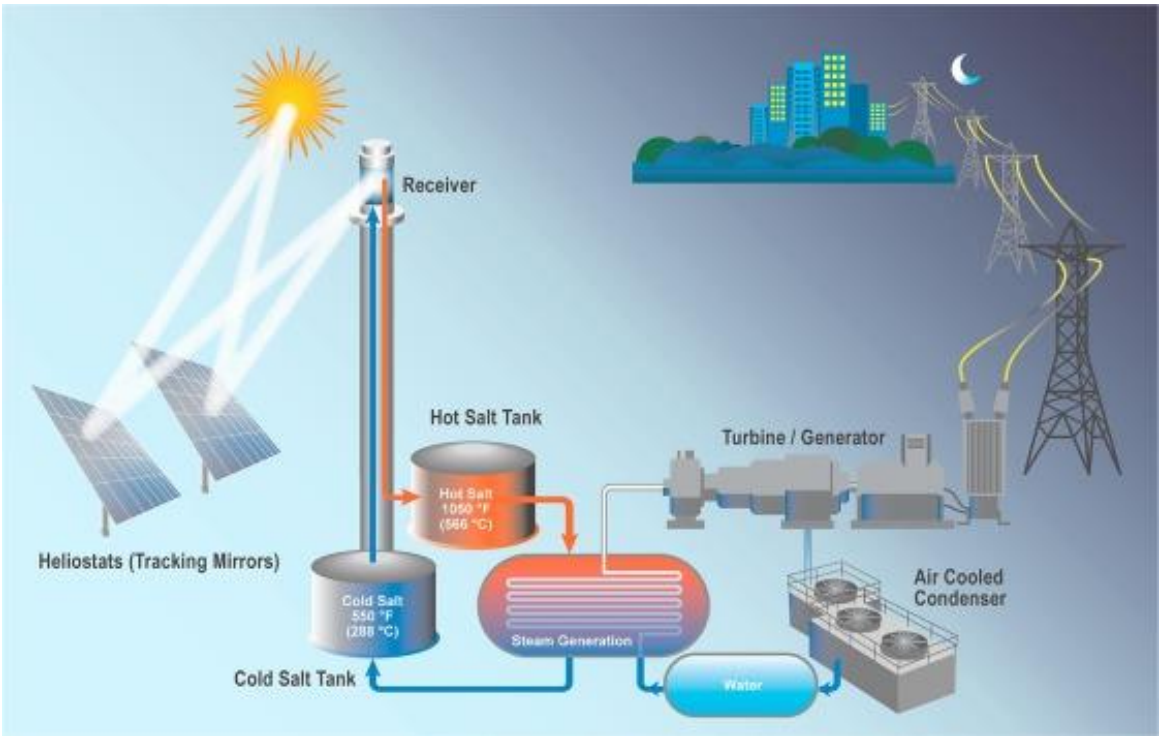

Figure 9 Schematic showing basic arrangement of solar tower system

The HTF used in solar tower technology is molten salt which can be heated to temperatures as high as 550^{o}C. The HTF is usually molten nitrate salts which help to

generate energy around the clock. Molten salt is an ideal heat capture medium because it maintains a larger operating temperature range in its liquid state allowing the system to operate at low pressure for enhanced and safe energy capture and storage (Agyekum and Velkin, 2020).

These systems can either be direct or indirect. The direct steam system does not have a thermal energy storage fitted with it. The thermal energy harnessed is directly used for steam production. Indirect systems have a thermal energy storage system that allows the production of electricity even when the sun is not shining.

Figure 9 shows a schematic of a solar tower CSP plant. This technology utilises liquid molten salt as both the energy absorption and the storage medium. Systems fitted with Thermal Energy Storage have the ability store some of the energy collected as thermal energy. The stored energy is used to produce steam for electricity generation when need arises. (Agyekum and Velkin, 2020).

Figure 10 Khi 100MW solar power plant, South Africa. (source: https://www.pinterest.com/pin/213850682276597153/)

Notable solar tower CSP developments include Yumen 100MW in China, Huanghe Qinghai 135MW also in China and Crescent Dunes 110MW solar energy plant in Nevada United States. Africa also has seen development of two solar tower power projects. These

are Redstone 100MW in, Khi Solar One in south Africa and Noor 3 150MW in Morocco. Likana Solar Energy Project currently under development in Chile is set to be one of the biggest solar tower power plants with a net turbine output of 390MW. Khi Solar One is shown in Figure 10.

2.3.5 Dish-Engine CSP systems

A solar dish-engine system converts solar energy into electricity by means of a heat engine. In this type of CSP system a large reflecting parabolic dish shaped mirror directs and concentrates sunlight onto a thermal receiver placed at its focal point (refer to Figure 11). The heat is then used to drive a heat engine that in turn drives a generator coupled to it to produce electrical energy. The major parts of this type of CSP system are the solar concentrator and power conversion unit. The solar concentrator is mounted on a tracking system that follows the position of the sun throughout the day to enable highest performance.

The power conversion unit comprises the receiver, heat engine and generator. The heat absorbed by the receiver is used to drive a heat engine couple to a generator. The most common type of heat engine used today in dish/engine systems is the Stirling engine. Stirling engine generator is a piston engine containing a gas that operates on a regenerative thermodynamic cycle transforming heat into mechanical energy. This type of engine is driven by the fluid heated by the receiver to move pistons and create mechanical power. The mechanical power is then used to run a generator to produce electricity (Nelson, 2020).

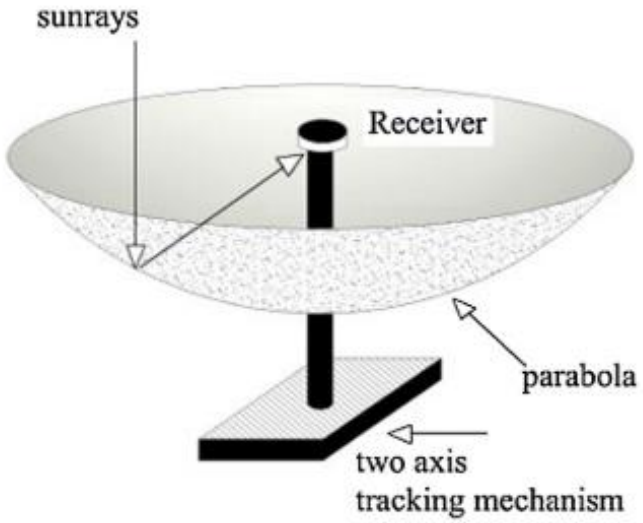

Figure 11 Parabolic dish collector (Ngoc et al., 2013)

According to Solar PACES (2021), there are only two Dish/Engine systems that have ever been operated commercially. One was the 1.5MW Maricopa Solar Plant in the United

States of America (USA). The plant has 60 parabolic dishes seating on 15 acres of land. The other is the 1.5MW Tooele army Depot Solar Project (shown in Figure 12) also in the USA. This plant comprises of 429 dishes with each dish having an Aperture area of 35m^2 and capacity of 3.5KW sitting on 17 acres of land. Both plants use the Stirling engine as the heat engine. It also should be noted that both plants are non-operational. Solar dish/engine CSP systems are the least deployed among the four main CSP technologies. Appendix 10 shows how the four CSP technologies compare against one another.

Figure 12 Tooele army depot solar dish/engine CSP plant (source: https://galvanizeit.org/project-gallery/stirling-solar-array-tooele-army-depot)

2.5 Key Sizing and Design Considerations in CSP Design.

There are several key factors that need to be seriously considered when sizing a CSP system. Design Point DNI, Solar Multiple (SM), Capacity Factor (CF), thermal storage hours as well as type of storage employed, environmental impact and costs are some of the most important factors.

2.5.1 Design DNI

The Handbook of Energy (2013) defines Direct Normal Irradiation as:

''*The amount of solar radiation received per unit area by a surface that is always held perpendicular (or normal) to the rays that come in a straight line from the direction of the sun at its current position in the sky.''*

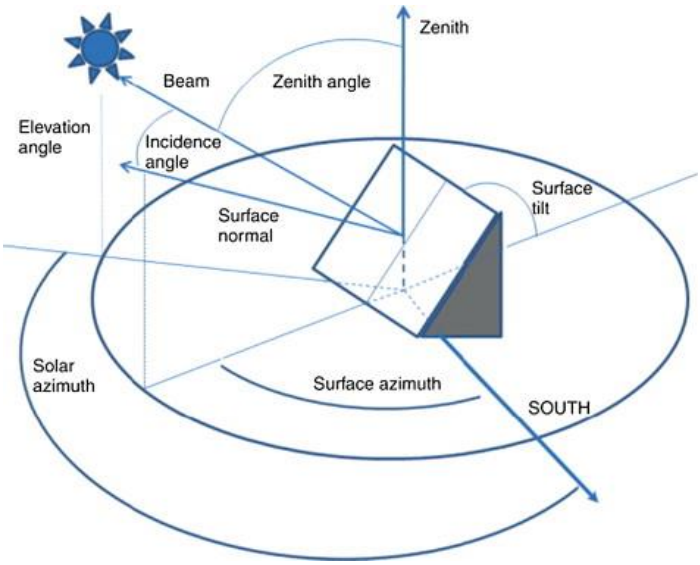

Figure 13 Common terms used to describe solar irradiance (Ngoc *et al.*, 2013 p. 409)

DNI is the first solar requirement that must be assessed before any developments of a CSP plant are made. Even though solar irradiance is an abundance resource on earth, most countries do not receive the required amount of DNI for CSP. CSP plants are typically favoured in countries within the sun belt region. The sun belt region lies between 40 Degrees North and south of the equator. The Sun belt region comprises the Middle East, North Africa, South Africa, India, the Southwest of the United States, Mexico, Peru, Chile, Western China, Australia, southern Europe and Turkey (IRENA, 2013, p.3).

Studies done by the International Renewable Agency suggest that a DNI of more 2000 kWh/m^2-yr is required to develop CSP power plants that are cost effective. However, the agency also mentions that there is no reason why CSP systems would not work at values slightly lower than 2000. Figure 13 shows the angles used in defining the solar irradiance on a surface. Zenith angle, incidence angle, elevation angle, surface and solar azimuths are shown on the figure. The zenith angle is the angle between the sun and the vertical. The zenith angle is similar to the elevation angle, but it is measured from the vertical

rather than from the horizontal. Solar Azimuth angle defines an angle that represents how many degrees from the exact south-facing direction surface is. Solar azimuth depends on location, date, time and time zone.

2.5.2 Solar Multiple

The National Renewable Energy Laboratory defines solar multiple as the actual size of solar field relative to that which would be required to reach rated electrical capacity at design point. A solar multiple of more than unity (1) is usually required to ensure effective utilisation of the generation capacity of the power block. Typically, a solar multiple of 1.3 or higher is considered good enough for systems without energy storage while a solar multiple of 2 or higher is considered good enough for systems having six hours or more of thermal energy storage (IRENA, 2019).

The solar multiple normalises the size of the solar field with respect to the power block. A system having a solar multiple of 2 implies that the solar field has a size twice that needed to capture the thermal energy required to operate the power block at its design capacity. Solar multiple, DNI and TES hours are interlinked (refer to Figure 14). The excess solar energy collected may be dumped or stored as thermal energy by a TES system for use at a later stage.

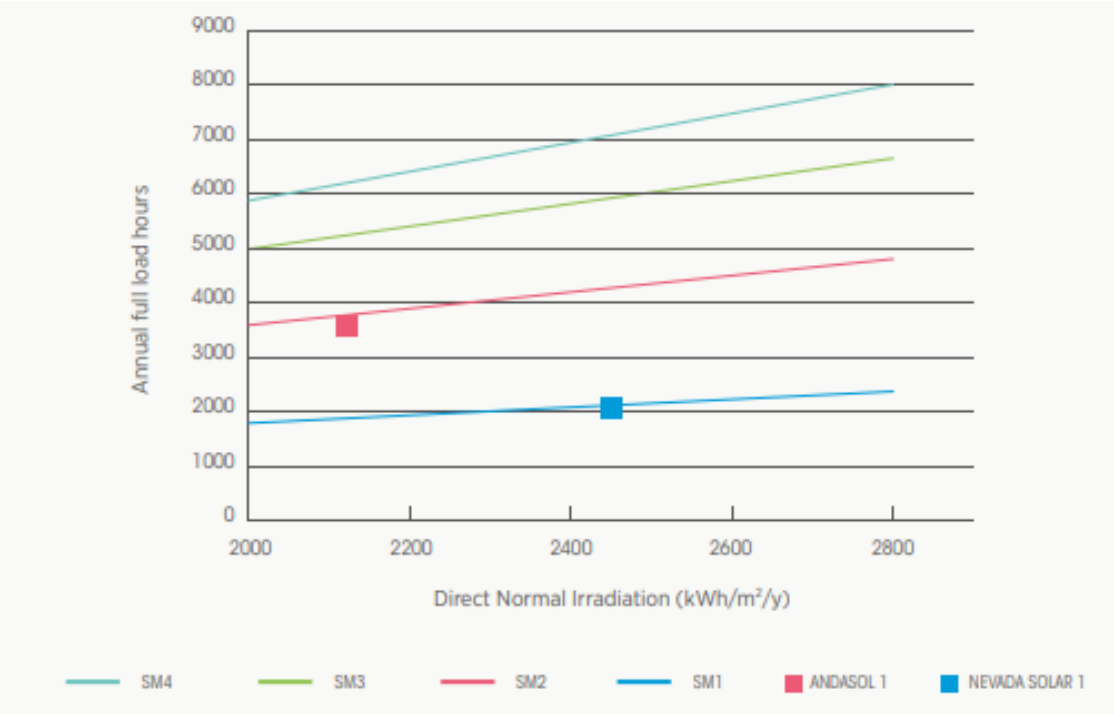

Figure 14 Projection of Annual full load hours as a function of DNI and Solar Multiple (SM). Sourced from (Santos *et al.*, 2018 p. 20)

2.5.3 Capacity Factor

The capacity factor compares the actual energy generated to the rated capacity of plant. It is calculated for longer spans (typically years). It is defined by equation 1.

$$Capacity\ factor = \frac{Actual\ emergy\ generated(MWh)}{Rated\ Capacity(MW)xTime\ period(h)} \quad (1)$$

In CSP system, capacity factor is mainly dependant on weather a system has thermal energy storage or not. While thermal energy storage increases capital costs, it allows higher capacity factors to be achieved. Thermal energy storage allows generation to be dispatchable even when the sun is not shining. It can also allow the maximum utilisation of generation capacity at peak periods of demand. Capacity factor can also be increased by increasing the solar field size relative to the power block capacity (IRENA, 2012).

2.5.4 Power Block

Commercially deployed Solar Tower, Linear Fresnel and Parabolic Trough CSP Systems employ steam turbines for power generation while solar dish systems commonly utilise Stirling heat engines for the same purpose. In Solar Tower, Fresnel and Parabolic CSP plants, the aim is to harness enough heat energy to produce steam which in turn is used in a Rankine cycle to produce electricity.

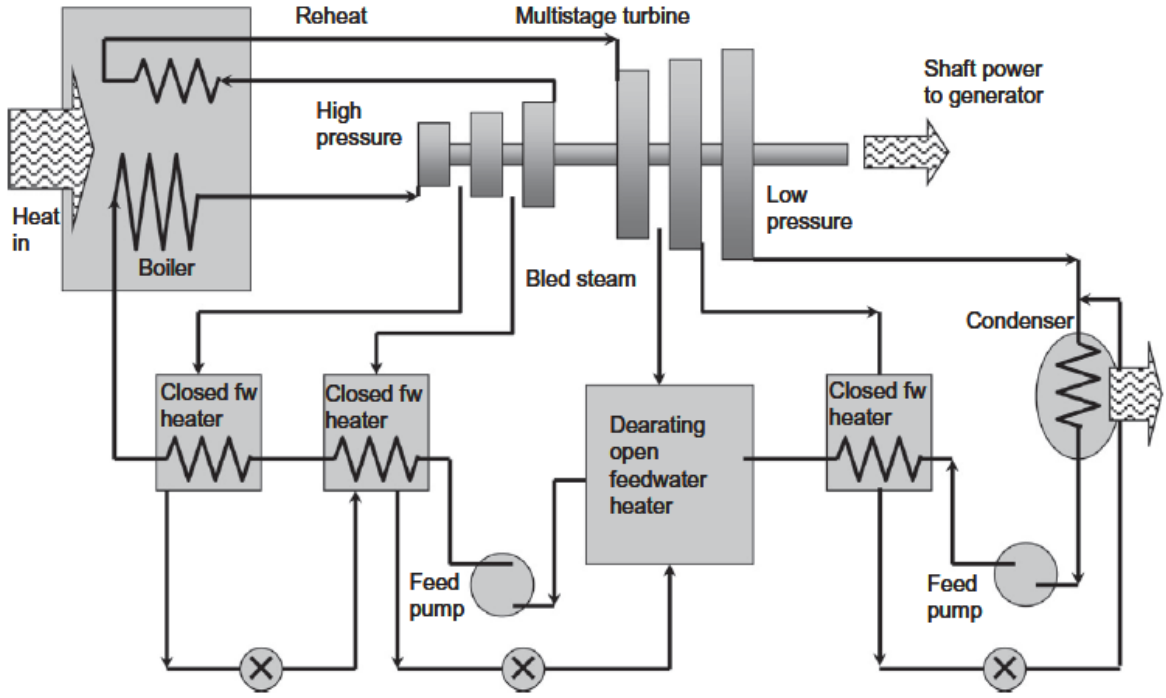

Figure 15 Steam turbine plant configuration for CSP systems (Lovegrove and Pye, 2012 p. 45)

A Rankine cycle begins by compressing feedwater to a high pressure, typically 10Mpa. Then the feedwater is heated using the heat from the HTF in a boiler (or via a heat

exchanger) to generate superheated steam. The generated steam is expanded to a lower pressure by passing it through a configuration of turbines coupled with an electricity generator. After flowing through the turbine, the low-pressure steam is condensed via cooling towers and the cycle begins again. To improve efficiency of the system in a practical system, steam can be bled at various stages from the turbine to preheat the feedwater before it enters the boiler. Efficiency could also be improved by the use of reheating stages as shown in Figure 15 which shows a typical layout of a steam turbine system. In the reheating stage, steam is bled from the boiler at intermediate pressure and fed in the boiler before being used to drive a secondary low pressure turbine (Lovegrove and Pye, 2012).

In practice, the amount of liquid condensing within the steam turbine is kept to a minimum to avoid erosion and pitting of the turbine blades. Lovegrove and Pye (2012) emphasize that the vapour must be sufficiently superheated before the expansion stage of the Rankine cycle.

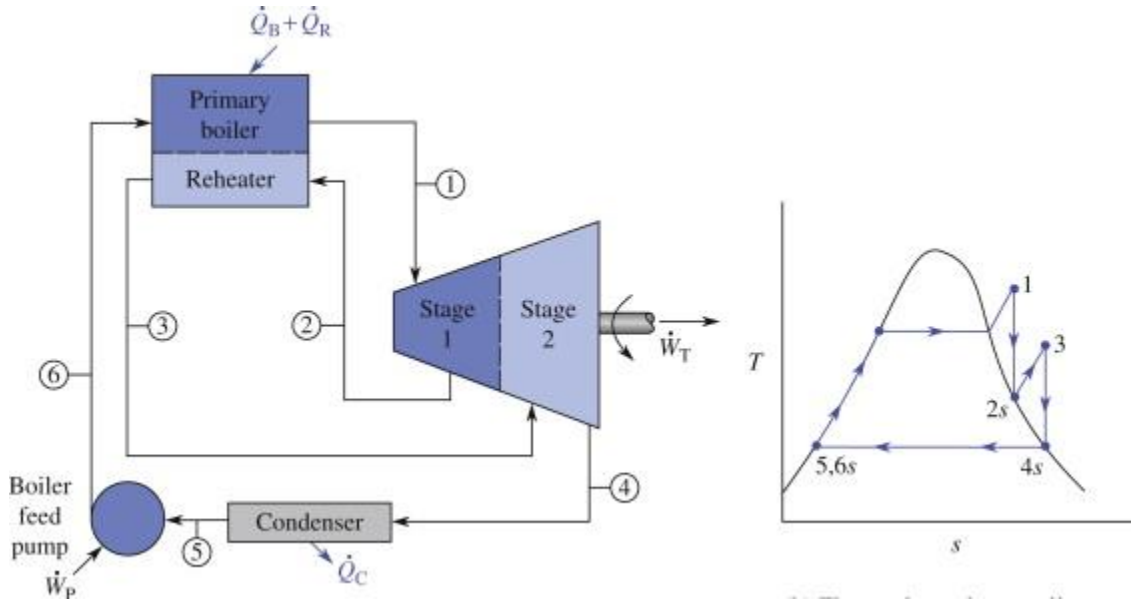

Figure 16 Equipment layout of Rankine cycle (left) and T-s diagram (right)

Efficient turbine systems work at temperatures close to 700°C at inlet to the turbine at efficiency of around 40%. While parabolic trough and linear Fresnel systems utilising high temperature synthetic oil as HTF are limited to a working temperature of 400°C. Solar tower and dish systems are able to achieve the high temperature needed to operate at optimal efficiency (Lovegrove and Pye, 2012).

2.5.5 Thermal Energy Storage

CSP systems are generally equipped with molten salt energy storage systems for improved, stable and scalable power output. A TES system will store energy in the form of heat which can later be utilized by the power block when the solar field is not harnessing enough thermal energy. Ordinarily, a TES system will harness energy from the solar field

from morning through afternoon to dispatch later in the day when the sun is not shining. TES systems can be direct or indirect. Direct TES system uses the same HTF as heat transfer fluid and thermal storage medium while indirect system uses different fluid as a thermal storage medium. Indirect storage systems tend to be more expensive as they require use of supplementary equipment such as heat exchangers to facilitate transfer of heat between the heat transfer fluid and thermal storage fluid (National Renewable Energy Laboratory, 2021a). Figure 17 and Figure 18 show the configuration of Direct and Indirect molten salt TES.

CSP systems make use of Sensible Heat Storage technology. Sensible heat storage is a commercially deployed type of TES that stores thermal energy by heating or cooling a storage medium without altering its state. The medium of storage can be liquid or solid. The storage capacity in these ranges from 10KWh/tonne to 50KWh/tonne while the efficiency ranges from 50% to 98%. The working temperature can be as low as -160^{0}C and as high as 1000^{0}C. The thermal capacity of storage is denoted by TES thermal capacity in MWht (IRENA, 2020). Thermal storage in CSP systems enable the technology to have a significant advantage over other renewable energy systems because they can deliver power at a stable, improved and scalable rate.

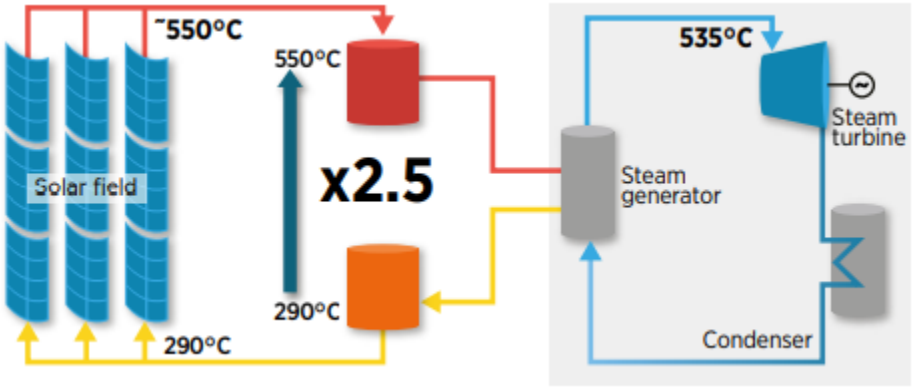

Figure 17 Direct molten salt TES (IRENA, 2020 cited *Archimede* Solar Energy, 2020 p. 56)

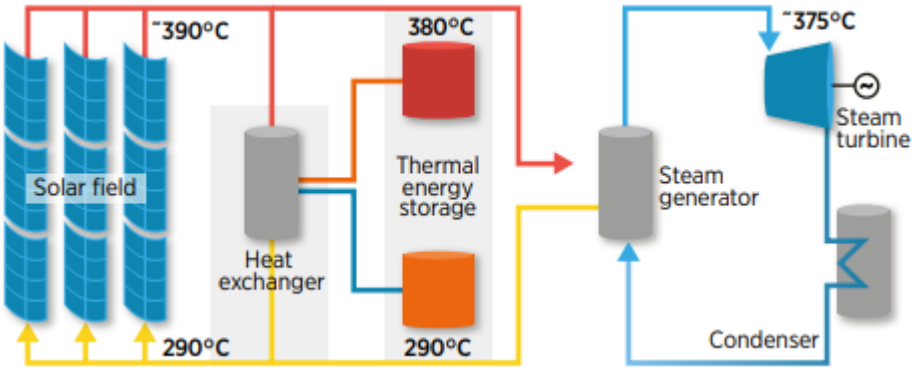

Figure 18 Indirect molten salt TES (IRENA, 2020 cited Archimede Solar Energy, 2020 p.56)

2.5.6 Hydrogen-Based Electrical Energy Storage

The storage of electricity produced from renewable energy sources continues to pose a significant challenge in the renewable energy sector. Over the last decade there has been efforts to utilise hydrogen as a means of storage for electricity. The most recent development is in United Arab Emirates' where Dubai Electricity and Water Authority (DEWA) has partnered with Siemens to produce green hydrogen using a fuel cell working on the principal Proton Exchange Membrane (PEM) technology. PEM electrolyzers are powered with energy from solar photovoltaics. The hydrogen produced is stored and utilised at a later time for re-electrification (Barhorst, 2016).

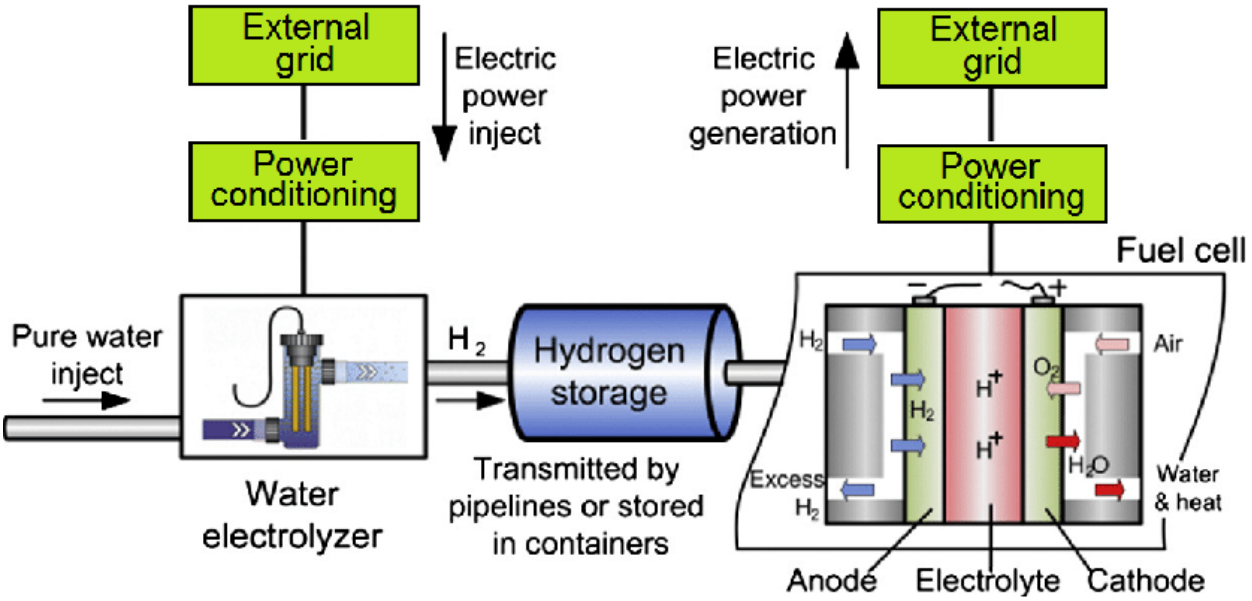

Figure 19 Concept of hydrogen storage (Zablocki, 2019)

The electrolyzer in the hydrogen system generates hydrogen from the excess electricity generated by the renewable energy source, which is in turn is stored in storage tank. The hydrogen is used to generate electricity through the fuel cell later to fill the gap between the supply and demand. The most significant advantage hydrogen-based electrical storage systems have over other well-known electrical energy storage technologies such as batteries and TES is its ability to provide storage for longer spans of time ranging from minutes, days or even weeks (Zablocki, 2019). Hydrogen-based storage is out of the scope of this work.

2.6 Key Environmental Impact Considerations

CSP systems use an insignificant amount of material once in operation. The emissions from the site are negligible in most cases. In construction however, these systems may have numerous impacts on the environment on which they are built. Thus, before embarking on a major CSP development comprehensive environmental impact assessment must be done in order to ensure the impacts associated with the project are avoided, reduced, mitigated or eliminated. Key environmental impacts are discussed in the following subchapters.

2.6.1 Land use

CSP systems need huge areas of land for development. The developer must pay attention in the planning phase and throughout the project in order to mitigate the effects on the environment, vegetation, fauna and habitat that may be hosted on the site. Ong *et al.* (2013) report in their findings that in USA parabolic trough, tower, dish and linear Fresnel CSP technologies require on average 9.5, 10,10 and 4.7 acres/MW respectively. CSP systems use larger area of land as compared to PV systems per MW output. Table 1 shows how the different PV and CSP systems rank in terms of land use based on four weighted averages.

Table 1 Land use requirements for PV and CSP Projects in the United States (Ong *et al*, 2013, p. V)

Technology	Direct Area		Total Area	
	Capacity-weighted average land use (acres/MW)	Generation-weighted average land use (acres/GWh/yr.)	Capacity-weighted land use (acres/MW)	Generation-weighted average land use (acres/GWh/yr.)
Small PV (>1 MW, <20 MW)	5.9	3.1	8.3	4.1
Fixed	5.5	3.2	7.6	4.4
1-axis	6.3	2.9	8.7	3.8
2-axis flat panel	9.4	4.1	13	5.5
2-axis CPV	6.9	2.3	9.1	3.1
Large PV (>20 MW)	7.2	3.1	7.9	3.4
Fixed	5.8	2.8	7.5	3.7
1-axis	9	3.5	8.3	3.3
2-axis	6.1	2	8.1	2.8
CSP	7.7	2.7	10	3.5
Parabolic trough	6.2	2.5	9.5	3.9
Tower	8.9	2.8	10	3.2
Dish Stirling	2.8	1.5	10	5.3
Linear Fresnel	2	1.7	4.7	4

2.6.2 Fauna, flora and ecosystems

CSP systems occupy huge acres of land. Hence their effect on fauna, flora and ecosystems must be considered carefully before and after development. Solar tower

systems may pose a danger to birds and insects. Birds may migrate from their normal habitat to areas that are more favorable where the effect of the CSP plant are not felt. In some cases, insects may be killed if they fly close to or into the line of focus of solar irradiance near the collectors. Vegetation that was once on the site before construction may be lost for good while that which remains may not develop as expected due the shed from the presence of the CSP power plant and its components (Tsoutsos, Frantzeskaki and Gekas, 2005).

2.6.3 Routine and accidental discharge of pollutants

This impact may arise during the operation phase. The coolants used in some indirect methods of cooling employed in solar thermal systems may contain anti-freeze and rust inhibitors which may pollute the environment in case of spillages or leakages. Additionally, the heat transfer fluids used in CSP systems contain glycol, nitrates, nitrites, chromates, sulfites and sulfates. These require controlled disposal and may cause water pollution if allowed to leak into the environment (Tsoutsos, Frantzeskaki and Gekas, 2005). Hence, extreme care must be taken when carrying out maintenance on HTF systems.

2.6.4 Noise

This impact may apply to parabolic dish systems that use heat engines such as the Stirling engines to produce electricity. The operation of Stirling engines may produce noise during operation, but this is very low as compared to noise made by fossil fuel-based engines (Tsoutsos, Frantzeskaki and Gekas, 2005).

2.6.5 Visual impacts

Visual impacts are pronounced in tower systems where solar irradiance is concentrated on to a central receiver. The concentration of solar irradiance on a small area results in the collector area appearing brighter in the sky thus causing a visual impact for humans and fauna near it. Thus, to mitigate this effect, these systems are typically deployed in locations with low population density in which visual intrusion is unlikely to be felt by the general public (Tsoutsos, Frantzeskaki and Gekas, 2005).

2.7 Cost of Concentrated Solar Power and Economic Trends

Costs associated with the different CSP systems can be measured and represented in several ways. Capital Expenditure (CAPEX) and Levelized Cost of Electricity (LCOE) are amongst the significant parameters that play a key role in the economics of CSP systems.

2.7.1 Capital Expenditure

Capital Expenditure represents the costs incurred before achieving commercial operation. This includes the costs related to the generation plant, site preparation, installation, infrastructure development and interest payments incurred during the construction phase.

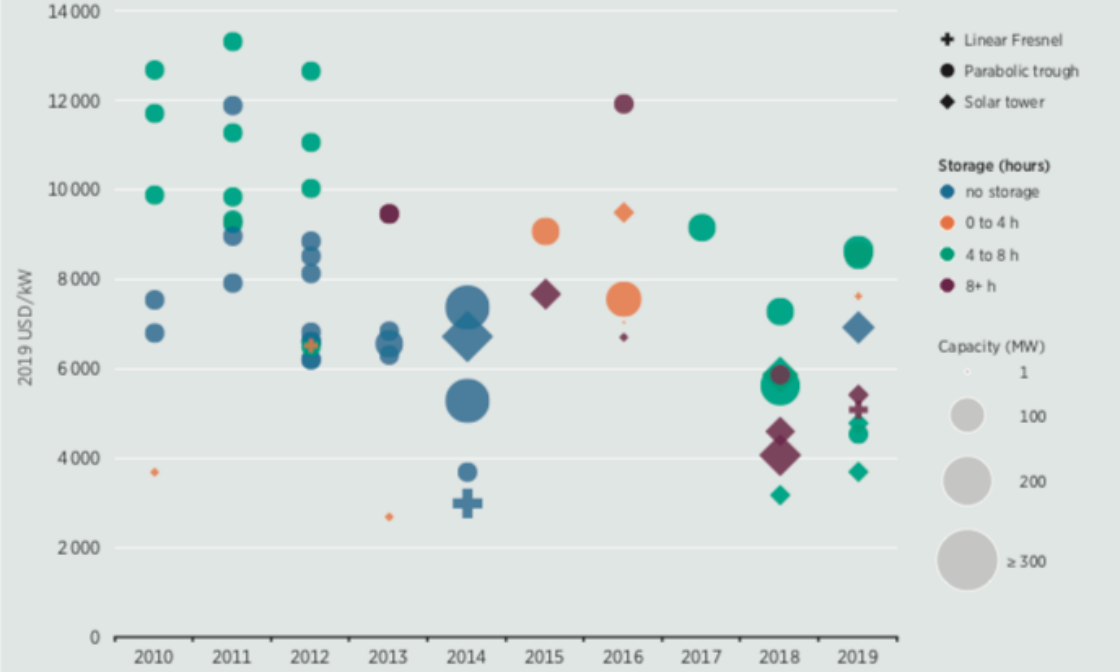

Figure 20 CSP total installed costs by project size, collector type and amount of storage, 2010-2019 (IRENA, 2020 p. 123)

According to latest statistics from IRENA, the capital costs for CSP projects commissioned in 2019 varied between $3040/KW and $8645/KW. This was nearly 16% higher than 2018 figures. The capital costs depend upon factors such as solar resource, technology and thermal energy storage hours. How these factors affect the CAPEX is highlighted in Figure 20. The most widely deployed CSP technology is the parabolic trough system. Investors may be drawn to venture into this kind of technology since the risk is well known. There is more reliable financial information about construction, maintenance and running costs of parabolic trough CSP systems.

2.7.2 Levelized Cost of Electricity

IRENA defines Levelized Cost of Electricity (LCOE) as the price of electricity required for a project where revenues would equal costs, including making a return on invested capital equal to the discount rate. A price of electricity that is above this value would result in better return on investment while a price below LCOE would result in a loss or lower return on investment. IRENA (2012, p. 3) suggests use of equation (2) to calculate LCOE.

$$LCOE = \frac{\sum_{i=1}^{n} \frac{I_t + M_t + F_t}{(1+r)^t}}{\sum_{t=1}^{n} \frac{E_t}{(1+r)^t}} \qquad (2)$$

In the above equation, I_t represents expenditures in year, $M_t$represents the operations and maintenance expenditure in year t, F_t represents fuel costs in year t, r is the discount factor while n is the life of the system in years.

LCOE is a widely used measure in evaluation, modelling and policy development. It is based on a Discount Cash Flow (DCF) analysis. International Renewable Energy Agency stipulates that the LCOE is affected by the following.

- Initial investment cost
- Capacity factor and efficiency
- Design DNI
- Operation and Maintenance Cost
- Capital Cost

Solar resource and plant design decisions also have a resounding influence on LCOE of CSP plants. LCOE reduces as the Design DNI exceeds the optimal figures. For example, Spain, with base DNI value of 2100KWh/m^2/yr the LCOE reduces by 4.5% for every 100KWh/m^2/yr that the DNI supersedes 2100 (IRENA, 2012). The same source records that thermal storage and solar multiple affect the LCOE (refer to Figure 21). Thus, a parametric combination of thermal storage hours and solar multiple is vital to attain economically feasible figures of LCOE.

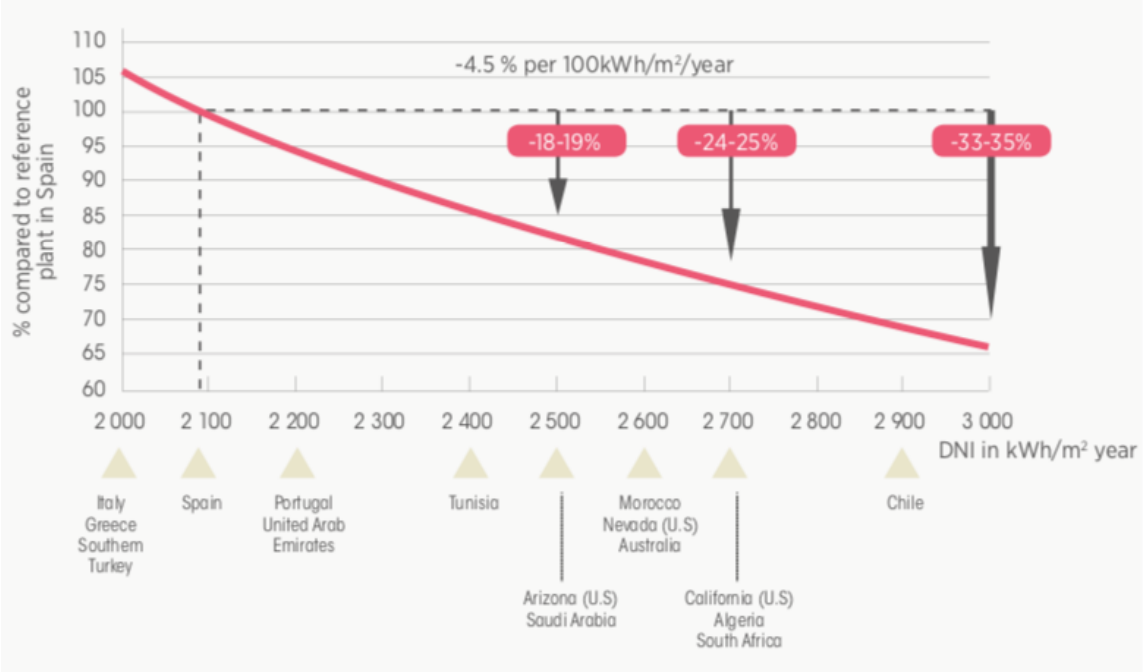

Figure 21 LCOE as a function of DNI for some parts of the world with good solar resource (IRENA, 2012 p. 31).

2.8 Concentrated Solar Power Modelling and Simulation Software Overview

There are several software packages that can be used to design, model and simulate CSP systems performance. The choice of software package one decides to use in their work solely depends upon familiarity with that software, cost and application. Some of the software packages available on the market today that are capable of modelling and simulating CSP system performance are summarized in Table 2.

Table 2 Summary of CSP software packages available on the market

Name	Developer, 1st release year	Key Applications	Cost
System Advisor Model	National Renewable Energy Laboratory (NREL), 2005	❖ Solar thermal processes (Parabolic, trough and linear Fresnel) ❖ Photovoltaic systems. ❖ Economic Analysis	Free
Integrated Simulation Environment Language (INSEL)	Jurgen Schumacher, release date unknown	❖ photovoltaic system simulation ❖ solar thermal system simulation ❖ dynamic building simulation	$1011 Single user educational license $2023 Single user commercial license $101 Student license
Transient System Simulation Tool (TRNSYS)	Thermal Energy System Specialists, LLC, 2017 (CSP tools incorporated)	❖ Solar thermal processes ❖ Emerging technology assessment ❖ Photovoltaic systems.	$5060 Commercial $2520 Educational
Green Energy Analysis tool (GREENIUS)	DLR, 2013	❖ Concentrating solar power plant system. ❖ Concentrating solar collectors for process heat ❖ Photovoltaic power systems ❖ Economic analysis	Free.

2.8.1 Green Energy Analysis tool (GREENIUS)

Greenius is a software tool developed by DLR Institute of Solar Research of German. The software tool can do performance calculations for several renewable energy systems. The key focus of the software is solar thermal power plants although other renewable energy systems have been incorporated in the software. Key application of the software includes the modelling and simulation of:

- ❖ Concentrating solar power plant system.

- Concentrating solar collectors for process heating.
- Photovoltaic power systems.
- Wind power systems.

The software is good for predictions of electricity yield and has proven to be extremely useful for feasibility studies. Economic modelling can also be performed in the software. Although not so popular, the software was launched in 2013 and is available for free (German Aerospace Center, no date)

2.8.2 System Advisor Model (SAM)

SAM is a software tool that was developed by National Renewable Energy Laboratory (NREL) with financial support from the United States Department of Energy. It is available for free and may be used for commercial as well as educational purposes. SAM can model many types of energy systems. Amongst these are the following:

- Photovoltaic systems.
- Battery storage systems (Lithium-ion, lead acid and flow batteries).
- Concentrating solar power systems (Parabolic, power towers and linear Fresnel).
- Concentrating solar based industrial process heat systems.
- Solar water heating.
- Fuel cells.
- Geothermal power generation.
- Biomass energy systems.
- High concentration photovoltaic systems.

SAM is also capable of financial modelling that includes analysis of levelized cost of electricity (LCOE, Power Purchase Agreements (PPAs), Lease agreements, Internal Rate of Return (IRR) to mention but a few.

In this project, I will use SAM version 29.11.2020. SAM is a trusted techno-economic tool that is used in the renewable energy industry by project managers, engineers, policy makers, developers and researchers. SAM has been available since 2007 and has undergone massive improvements since then, leading to its public use by over 130,000 users across the globe (National Renewable Energy Laboratory, 2021a).

2.8.3 Integrated Simulation Environment Language (INSEL)

INSEL is a block diagram-based simulation system that is suited for large and complex energy projects. It is also ideal for research. The software works in conjunction with MATLAB and Simulink features thus offering a vast collection of model components for a wide range of applications. INSEL can be used to perform the following analysis:

- photovoltaic system simulation.
- solar thermal system simulation.
- dynamic building simulation.
- Meteorological data simulation.

The software costs $1011 for single user educational user license and $2023 for single user commercial license. (INSEL, 2021)

2.8.4 Transient System Simulation Tool (TRNSYS)

TRNSYS is a graphic based software tool that can simulate the behavior of transient systems. The software package is capable of assessing the behavior of thermal and electrical energy systems. The software has a standard library that boasts approximately 150 models which include CSP based systems, wind turbines, pumps, multizone buildings to mention but a few. The package is used by Engineers, researchers, consultants and architects among an extensive network of users around the world. Key application of TRNSYS include the following:

- Solar thermal processes.
- Energy system research.
- Emerging technology assessment.
- Hydrogen fuel cell systems.
- Wind energy systems.
- Photovoltaic systems.
- Data and simulation calibration.

TRNSYS does not include financial analysis. The software costs $2520 and $5060 for the educational version and commercial version, respectively. It was developed by Thermal Energy System Specialists, LLC of United States of America. (Thermal Energy Systems Specialists, 2019)

3 Methodology

3.1 Approach

In this work, SAM software was used to model parabolic trough collector, solar tower and linear Fresnel Receiver CSP systems. SAM makes performance predictions and cost of energy estimations for power projects based on weather data, system design parameters, installation and operating costs that are specified as inputs to the models. The modelling steps taken in SAM are shown in Figure 22.

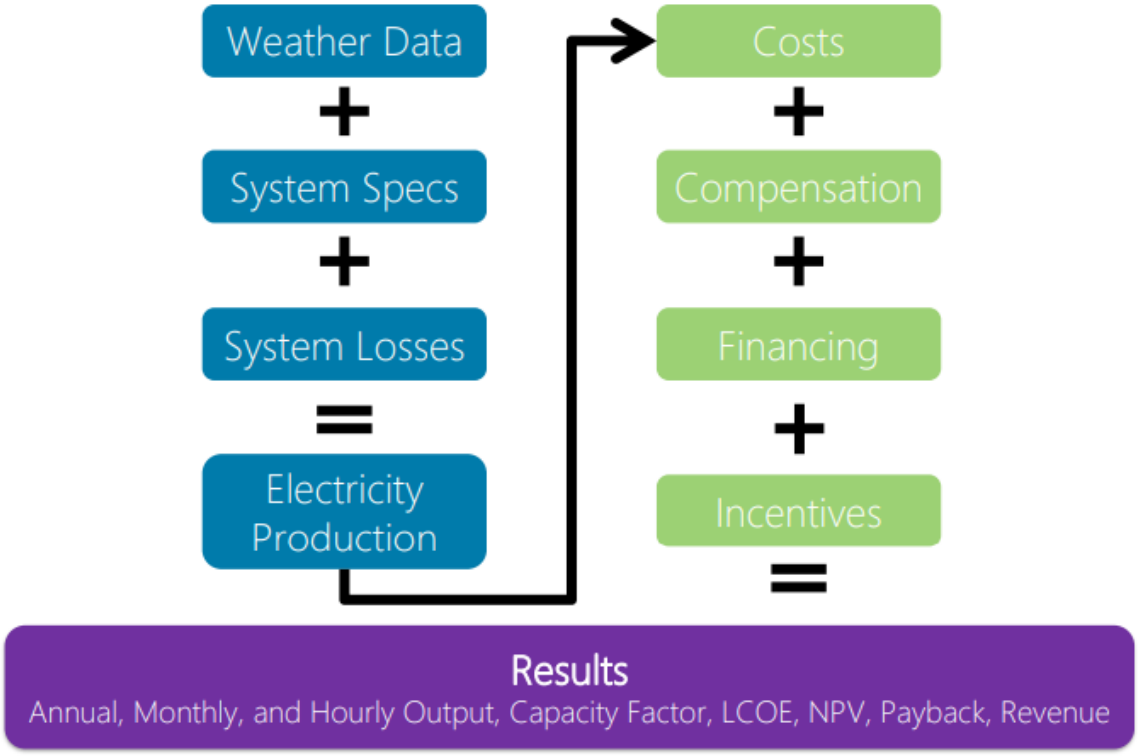

Figure 22 Modelling steps in SAM

The main aims of the methods employed in this work will be to:

1. Analyse the weather profile at the case study smelter plant in terms of solar irradiance.
2. Understand the nature of the case study smelter plant in terms of energy consumption and cost. This will involve the analysis of daily electricity consumption figures for the year 2020.
3. Analyse the practicability of using CSP technology with TES to supply power to the copper smelter while consideration of optimisation of design point DNI, Solar Multiple (SM) and TES hours.
4. Determine key economic performance metrics (Annual bill savings, Levelized Cost of Electricity and Net Present Value)
5. Compare the technical and economic metrics for each system in order to determine which system is feasible enough for the case study site.

It should be noted that all equations adopted in this methodology are sourced from the latest System Advisor Model software manual unless stated otherwise.(National Renewable Energy Laboratory, 2021a)

3.2 Case Study plant: Chambishi Copper Smelter Ltd.

3.2.1 Weather profile

The weather resource used in this analysis was downloaded from National Solar Radiation Database (NRSDB) of the United States of America. NRSBD is an online data base of weather files containing solar resource data from around the world. This was done by pinpointing the location of the case study site by use of latitude, longitude decimal coordinates (-12.656735,28102823). *Suffice to mention that the solar resource file will be the same for all three systems simulated in SAM*.

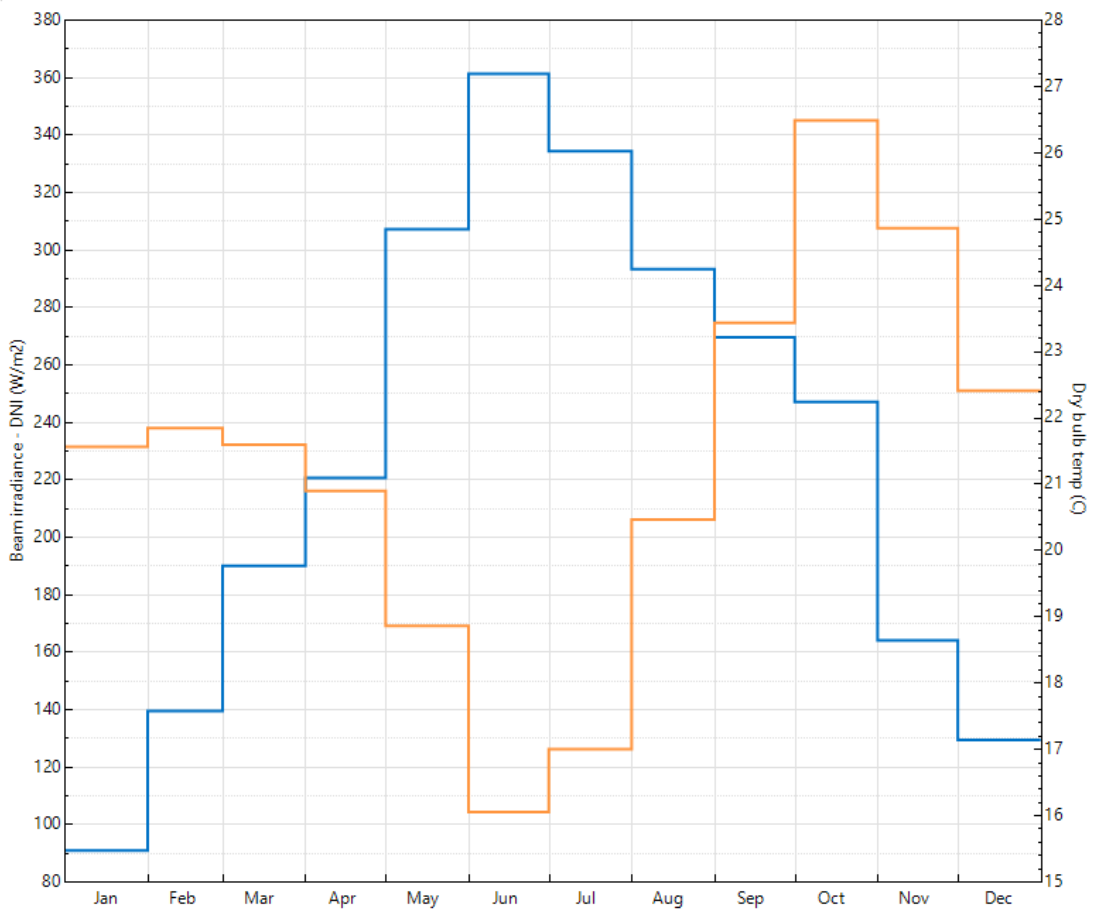

Figure 23 Average monthly DNI (blue line) and dry bult temperature (orange line) (National Solar Radiation Database (NRSDB))

The average monthly direct Normal Irradiance (DNI) and dry bulb temperature at the case study site is shown is shown in Figure 23. The average yearly DNI value for the site is 1925Kwh/m^2 while the average yearly GNI is 2145KWh/m^2. For a site to be technically feasible to host CSP plant, the yearly DNI average must be at least 1900 KWh/m^2

(Agyekum and Velkin, 2020). Thus, the case study site receives enough solar radiation to be considered for CSP installation.

3.2.2 Power Consumption

The case study is a copper smelting plant as mentioned in previous chapters. The plant imports electricity from the national grid, which is run by the state electricity supplier, Zambia Electricity Supply Corporation (ZESCO). Even though the law in Zambia allows independent power providers to sell power to the grid, the energy sector is predominantly run by the state. The average monthly consumption for the site in the year 2020 was 11.19GWh. A total of 15.26GWh was consumed in October. This value represents a quantity of electricity that is enough to provide power for approximately 49,000 households in the country for one month. The average urban household in Zambia consumes on average 312KWh in a month (United States Agency for International Development USAID, 2020). The total energy consumed in 2020 was 134.256GWh.

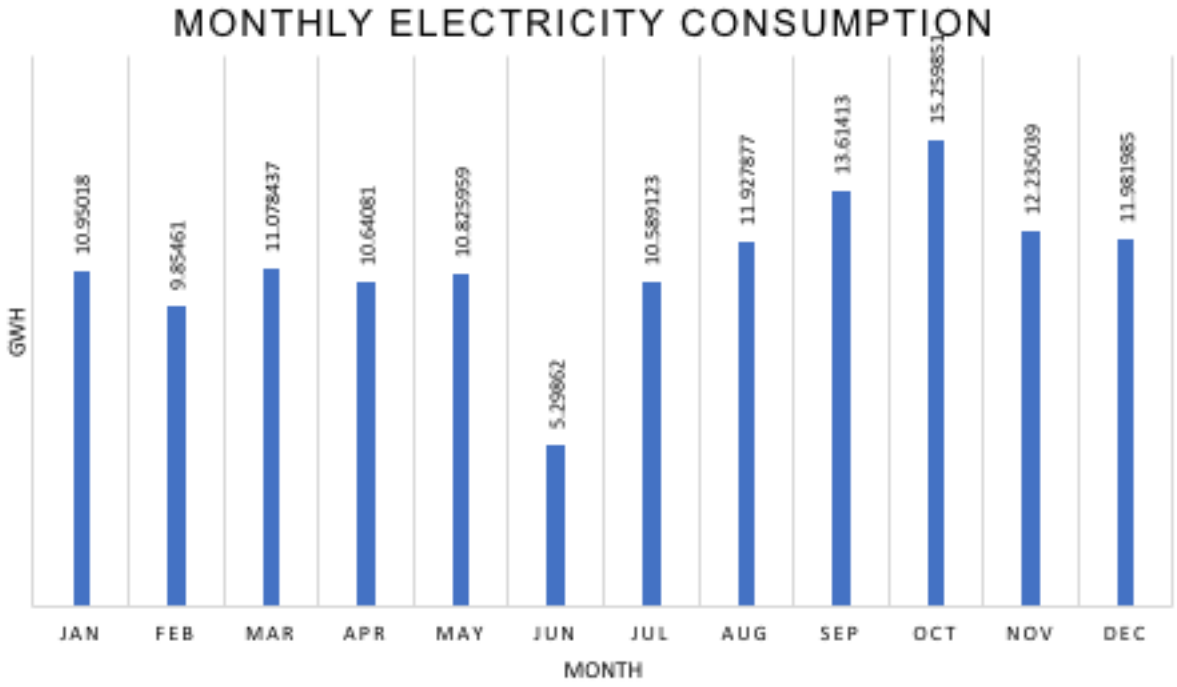

Figure 24 Monthly Electricity Consumption (MWh) for 2020

The monthly consumption for the year 2020 is shown in Figure 24. The graph shows a steep decline in the consumption between June and July. During this period the plant was shut down for annual maintenance. This maintenance takes place every year around June and July. The shutdown period lasted 42 days between those two months. Additionally, there are months in which weeks long maintenance shutdown are conducted depending on the performance of the overall plant. Such a month is February which had a low consumption relative to the months with normal operational consumption. A total of 8760 (1 entry per hour for 1 year) data points for the load were created and uploaded into

SAM software. The cost of electricity in the region costs an average of $0.044/KWh for businesses although exact costs of power to the mines is not publicly disclosed (Energy Regulation Board, 2019).

3.3 Solar Power Tower with Molten Salt Thermal Energy Storage

The system was designed and simulated in SAM software version 29.11.2020. Sizing of solar tower systems that utilize optimum thermal energy is important for ensuring reliability and cost reduction. Key design parameters such as solar multiple and thermal storage backup hours play a vital role in design (Jorgenson *et al*., 2013). The key parameters were optimized in order to simulate the best fit model for the site. Figure 25 shows the solar tower CSP schematic in SAM.

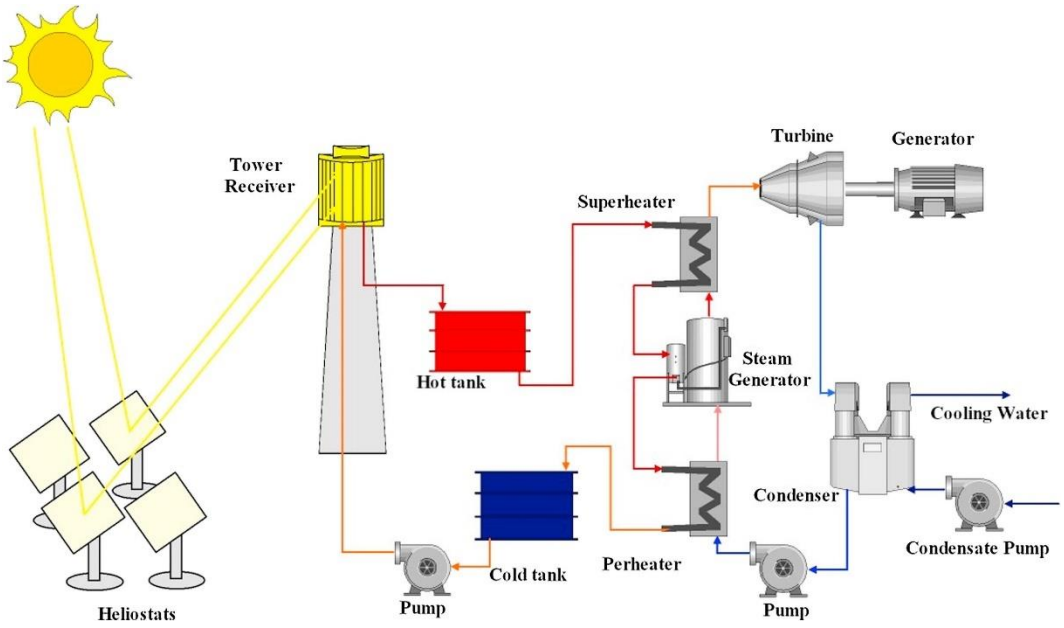

Figure 25 Solar Power Tower System in SAM

3.3.1 Power Block

In SAM, this is where the systems' nameplate capacity is defined. The name plate capacity for the power tower system is set at 50MWe design gross turbine output to produce an estimated net output of 45MWe. The conversion factor is assumed to be 0.9 (suggested by NREL). This chartered for the plant electrical demand as well as providing potential for export to the national grid. The estimated net output at design (nameplate capacity) is related to design gross power output and gross-to-net conversion by equation (3).

$$Estimated\ net\ out(MWe) = Design\ gross\ output(MWe)\ x\ Est\ gross - to - net\ CF \quad (3)$$

SAM takes into consideration thermal efficiencies. Thermal-to-electric conversion efficiency of the power cycle at the design point is represented as the cycle thermal efficiency while the cycle thermal power is that power required at cycle inlet for it to operate at baseline design conditions. These are related by equation (4).

$$cycle\ thermal\ power(MWt) = \frac{design\ turbine\ gross\ output(MWe)}{cycle\ efficiency} \quad (4)$$

3.3.2 Design Point DNI

NREL recommends use of a DNI of value at least 90% Cumulative Distribution Function (CDF). This value is practical to ensure that the receiver achieves thermal power rating more than 90% of the time (National Renewable Energy Laboratory, 2021a). The value was set at 900W/m^2 as shown in Figure 26.

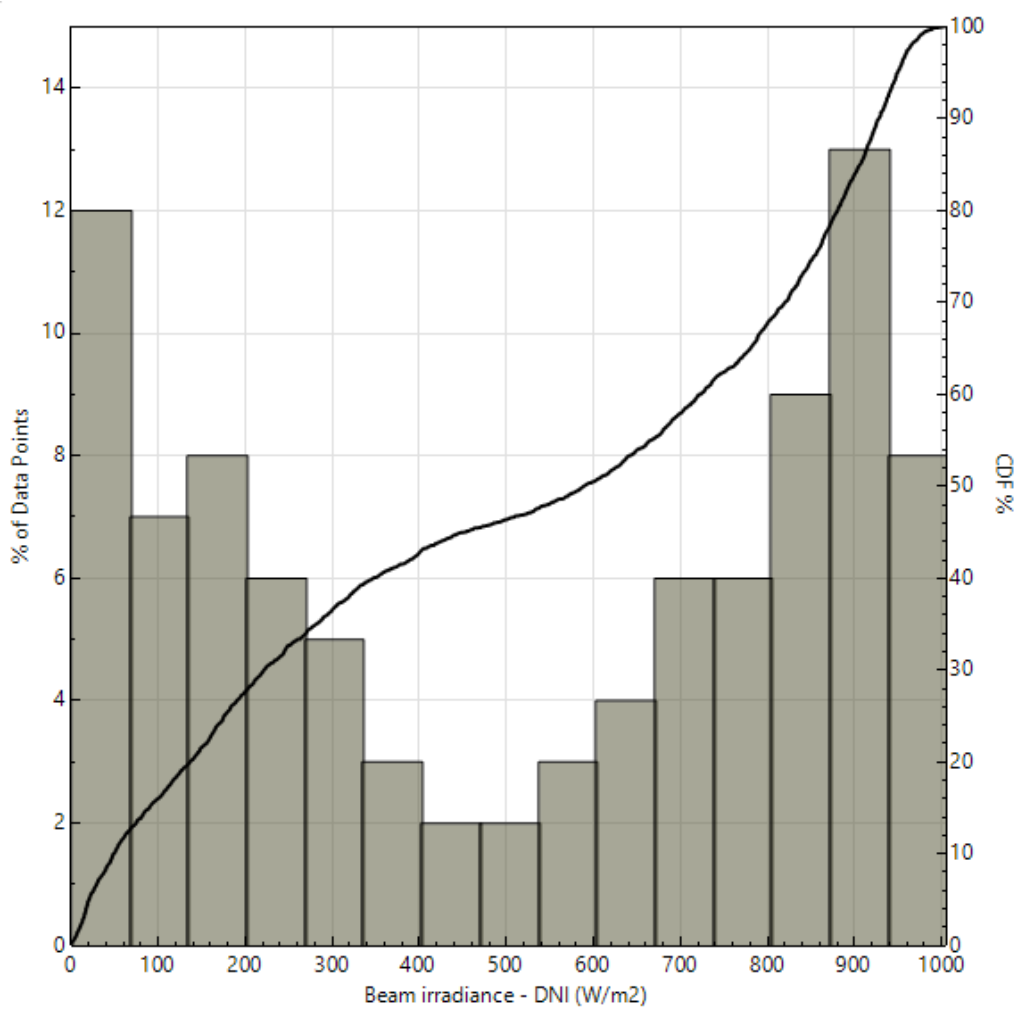

Figure 26 Cumulative Distribution Function of DNI values at the Case study site.

3.3.3 Solar Multiple

The Solar Multiple (SM) profoundly influences the overall size of the plant and the LCOE. Thus, it is imperative that an optimized value is used in the simulation. The optimisation is done via a parametric analysis in SAM. The result of this optimisation is shown in Figure 27. The optimisation shows that a SM of 2 provides the best LCOE.

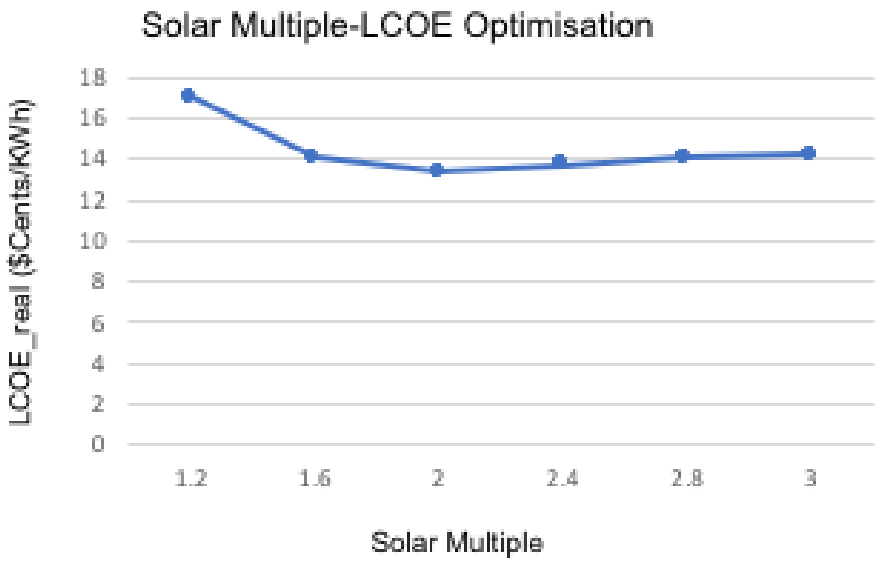

Figure 27 Solar Power Tower SM optimization

3.3.4 Heliostat Field and Layout

The average DNI was generated by SAM through use of exact longitude and latitude coordinates. the design point DNI was set as 900W/m^2. For design-point calculations involving solar irradiance, SAM uses the design-point DNI value with the sun position at noon on the summer solstice (June 21 north of the equator, and December 21 south of the equator). The layout of the heliostat field was optimized and reported after simulations (National Renewable Energy Laboratory, 2021b).

3.3.5 Tower and Receiver

The receivers' nominal thermal power is determined by the Solar Multiple (SM). SM is the ratio of the receiver thermal power to the cycle thermal power. For systems with no storage the solar multiple should be close to unity (National Renewable Energy Laboratory, 2021b).

$$receiver\ thermal\ power(MWt) = solar\ multiple\ x\ cycle\ thermal\ power(MWt) \quad (5)$$

The solar radiation incident (Q_{rec}) on the receiver aperture area (A_f) is given by the equation (6).

$$Q_{rec} = DNI.A_f\ .\eta_{field} \quad (6)$$

In the equation, η_{field} is the efficiency of heliostat field. The height of the solar tower, receiver-to-heigh ratio and receiver diameter are determined through parametric optimisation. The initial optimisation step size was 0.06. At total of 200 optimisation iterations were done with an optimisation convergence tolerance of 0.001.

3.3.6 Heat Transfer Fluid (HTF)

The heat transfer fluid used in the simulation was Hitec solar salt (60%NaNO3 40%KNO3). At a solar multiple of 2 (the default setting before any simulation is done), the receiver thermal power was set 242.7MWt. The hot HTF temp is 574.0^{o}C while the cold HTF temp is 290^{o}C. Refer to Appendix 11 for list of available HTF fluids. The receiver heat transfer tubes have an outer diameter of 40mm with thickness 1.25mm. the coating emittance of the tubes Is 0.88 while the coating absorbance is 0.94. The piping material used in this simulation is stainless AISI316.

3.3.7 Power Cycle

The power cycle in CSP systems operates based on the Rankine cycle. The main operation components of this cycle are the steam turbine, preheater, evaporator, superheater and condenser. Given a power output *w*(t) from the power block per hour in a time step Δt, the annual electricity generation (E) is given by the equation (7).

$$E = \sum w(t)\Delta t \tag{7}$$

The efficiency of the power block is defined as the ratio of power generation(*E*) and the heat input from the molten salt. Typically, the efficiency is around 42%. Equation (8) gives the annual solar-to-electricity efficiency. (Chen, Rao and Liao, 2018).

$$\eta = \frac{E}{Q_{solar}} \tag{8}$$

3.3.8 Thermal Energy Storage (TES)

Thermal storage is defined by two terms in SAM. These are Full load hours of storage and Solar field hours of storage. According to National Renewable Energy Laboratory (2021b), full load hours of storage refer to the nominal thermal storage capacity expressed in hours at full load which is basically the number of hours the storage system can supply energy at the design point of the cycle. Solar field hours of storage refer to the nominal thermal storage capacity expressed in hours of the solar fields design thermal power output (National Renewable Energy Laboratory, 2021a). A parametric optimisation was done by setting full load hours and SM as inputs while LCOE was set as the output parameter. The results of the optimisation strongly suggested choosing a SM was 2 and 12 TES hours (refer to Figure 28).

$$solar\ field\ hours\ of\ storage = full\ load\ hours\ of\ storage\ x\ solar\ multiple \tag{9}$$

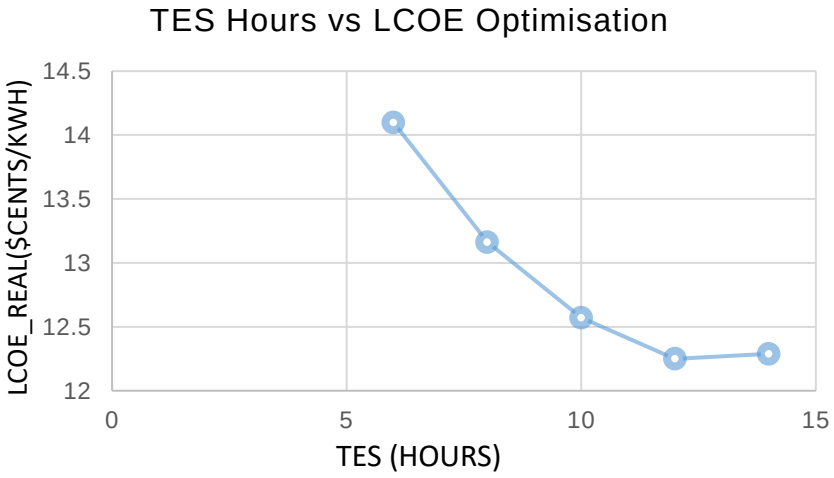

Figure 28 Solar Power Tower TES hours optimized against LCOE at a SM pf 2.5

A summary of system parameters used in SAM for modelling ST system is given in

3.4 Molten salt Linear Fresnel Receiver (LFR)

A procedure similar to that followed in simulating a molten salt solar tower system was employed for the molten salt linear Fresnel system. Optimized values of DNI, solar multiple and full load hours were used to ensure the resulting system has the best fit results as regards to cost and performance. The molten salt linear Fresnel commercial model in SAM constitutes the solar field, optional thermal energy storage system, optional auxiliary fossil backup system, steam Rankine power cycle, heat rejection system, feedwater pumps, and plant control system. Key outputs from the model comprises financial metrics and detailed performance (National Renewable Energy Laboratory, 2021b).

3.4.1 Power Block

The power cycle converts thermal energy collected by the receivers to electric energy. The nameplate capacity of the plant is determined by design gross output and the estimated gross-to-net conversion factor.

$$Estimated\ net\ out(MWe) = Design\ gross\ output(MWe)\ x\ Estimated\ gross-to-net\ CF \quad (10)$$

The estimated gross-to-net conversion factor is the ratio of the electrical energy delivered to the grid to gross output. SAM calculates this factor. The estimated net capacity was 45MWe, taking the estimated gross-to-net conversion factor as 0.9.

3.4.2 Solar field

SAM calculates the total required solar field aperture area and number of loops based on the value of solar multiple entered. Thus, it is imperative that the value of SM chosen is an optimized one associated with the most economic solar field size. Figure 29 shows the optimisation of SM considering LCOE. The best solar multiple chosen for our system was

2.5. A solar multiple of 3 is not economical because it implies use of a large solar field which results in extra cost. Caution must be taken when choosing a value for SM.

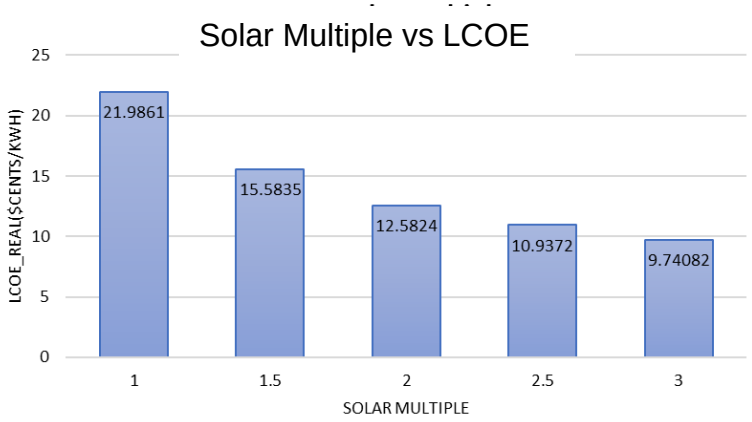

Figure 29 Solar multiple optimizations for LFR

3.4.3 Collector and Receiver

Several terms are used to define some of the inputs used in defining the collector geometry (refer to Figure 30).

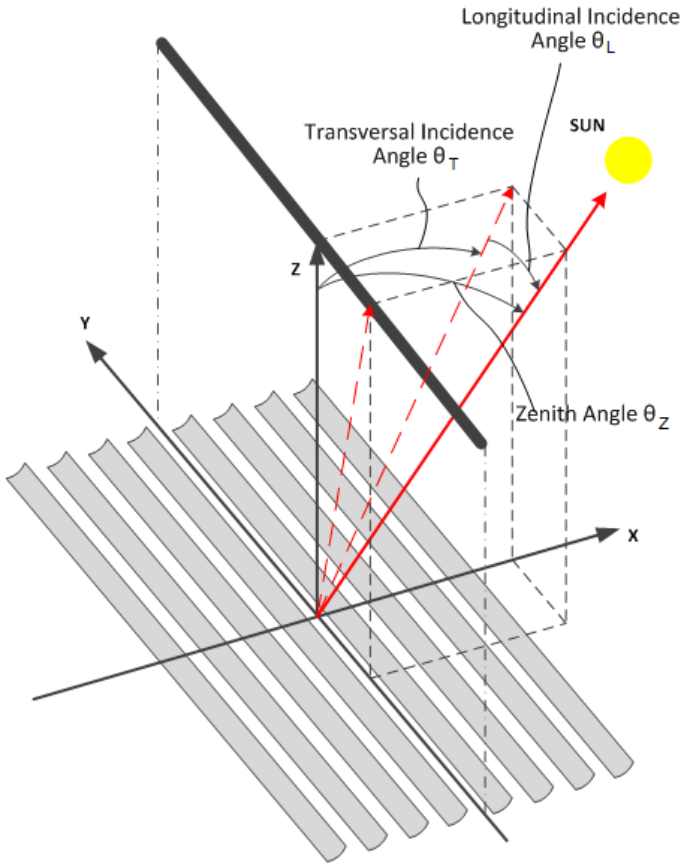

Figure 30 Solar position given by zenith, transversal and longitudinal angles (National Renewable Energy Laboratory, 2021a).

The definitions below are derived from (National Renewable Energy Laboratory, 2021b).

Reflective aperture area: this is the area for collector module. Together with collector optical efficiency and the solar irradiance value, it determines the total thermal energy that is incident on the receiver modules.

Length of collector module: this refers to length of the collector module along the axis of the receiver. The length of the collector module is useful in determining the thermal losses (W/m).

Length of crossover piping in a loop: this is the length of piping used to link collector roles in a loop. These may add to inertia as well as thermal losses.

Collector Azimuth angle(degrees). The collector azimuth angle is the angle between the primary axis of the LF collector and the North-South axis. It is negative if the collector is rotated in the anticlockwise direction and positive in the clockwise direction.

Traction error derate: this is primarily useful when it comes to determining the total optical efficiency of the system. The tracking error derate is simply fixed optical loss representing collector tracking error.

Solar weighted mirror reflectivity: this is the optical loss fraction coupled with mirror reflectivity while not considering soiling on the mirrors.

Dirt on mirror derate: the optical loss fraction coupled with accumulation of soil on the mirrors (National Renewable Energy Laboratory, 2021b).

Optical efficiency: the optical efficiency is best defined by the equation (11).

$$optical\ efficiency = \frac{total\ thermal\ energy\ absorbed\ by\ reciever}{DNI\ x\ Actual\ Aperture\ Area(AAA)} \qquad (11)$$

Collector incidence angle table.

This table allows the solar field efficiency as a function of the longitudinal incidence angle and the transversal solar incidence angles. These two angles are shown in Table 3 below. Default values in SAM were adopted.

Table 3 Collector incidence angle table

	0	10	20	30	40	50	60	70	80	90
0	1	0.97894	0.95382	0.94864	0.91162	0.86104	0.7036	0.48456	0.23609	0
10	0.97791	0.95732	0.93275	0.92768	0.89148	0.84202	0.68806	0.47386	0.23087	0
20	0.92189	0.90247	0.87932	0.87454	0.84041	0.79378	0.64864	0.44671	0.21765	0
30	0.83049	0.813	0.79214	0.78784	0.75709	0.71509	0.58433	0.40242	0.19607	0
40	0.70119	0.68642	0.66881	0.66518	0.63922	0.60375	0.49336	0.33977	0.16554	0
50	0.5336	0.52236	0.50896	0.50619	0.48644	0.45945	0.37544	0.25856	0.12598	0
60	0.32563	0.31877	0.31059	0.30891	0.29685	0.28038	0.22911	0.15779	0.07688	0
70	0.1173	0.11483	0.11188	0.11128	0.10693	0.101	0.08253	0.05684	0.02769	0
80	0.01103	0.0108	0.01052	0.01046	0.01006	0.0095	0.00776	0.00534	0.0026	0
90	0	0	0	0	0	0	0	0	0	0

3.4.4 Thermal Energy Storage (TES)

This is expressed by the number of storage hours of thermal energy delivered to the power block at the rated thermal input level. Thermal energy capacity (C) in SAM is calculated by equation (12).

$$C = \frac{W_{des\_gross}}{n\_des} x\ t_{full\_load} \qquad (12)$$

W_{des_gross} is the flow rate of the HTF in the collector. t_{full_load} is the total number of full load hours of thermal storage. n_des is the design thermal efficiency.

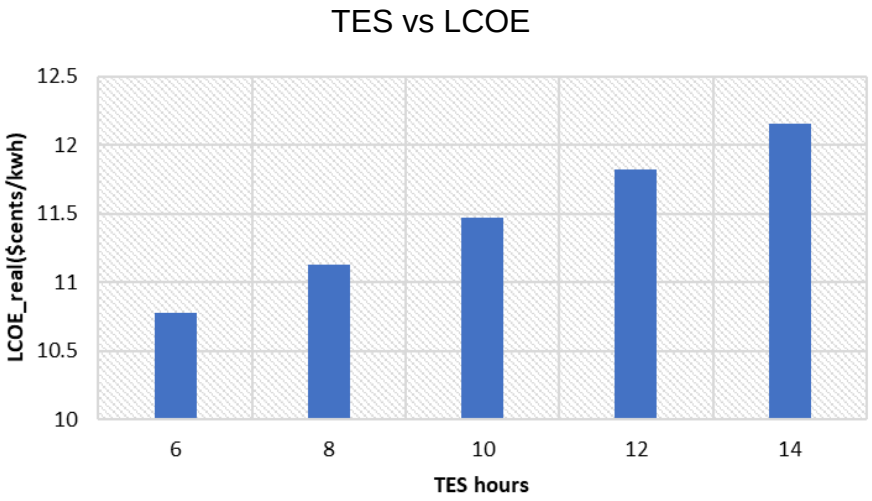

Figure 31 TES optimization

The optimized (see Figure 31) TES hours chosen for LF system is 10 hours. The HTF used in the modelling of the linear Fresnel system was Hitec solar salt. Hitec solar salt

has a maximum operating temperature of 593^{o}C and minimum operating temperature of 238 ^{o}C. The fluid density and specific heat capacity are 1829.38kg/m^{3} and 1.51335kj/kg-k respectively.

Summary of system parameters used in SAM for modelling LFR system is given in Appendix 2.

3.5 Parabolic Trough Systems

The key systems to be considered in SAM under parabolic trough model are shown in Figure 32

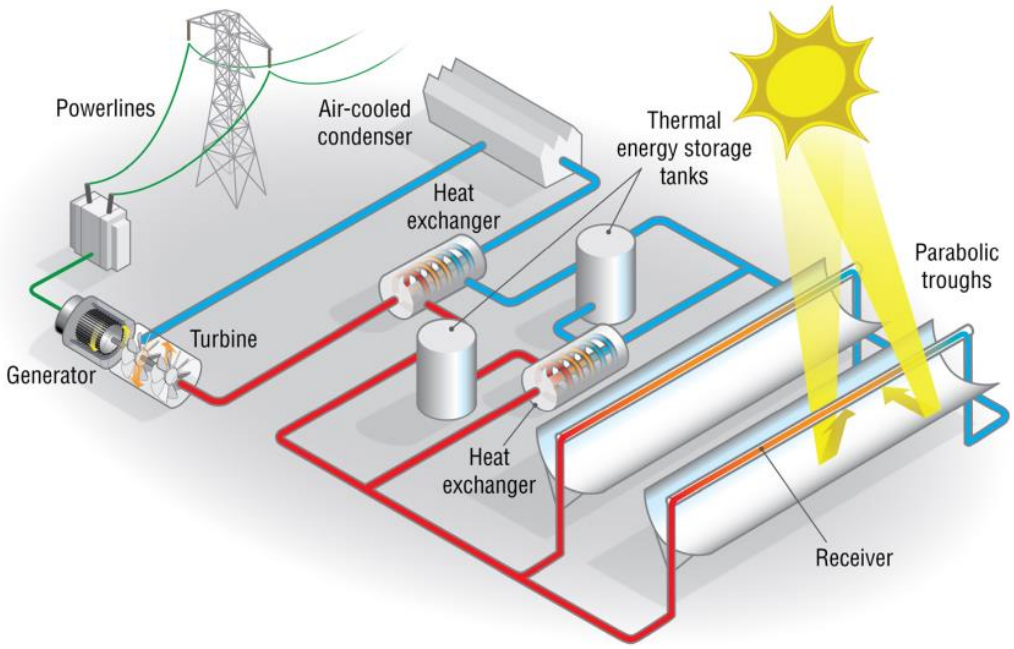

Figure 32 Representative model of parabolic trough system with TES.

3.5.1 Power Block

The name plate capacity of the parabolic trough system is related to the design gross output and gross-to-net conversion factor by the equation (3).

$$Estimated\ net\ out(MWe) = Design\ gross\ output(MWe)\ x\ Estimated\ gross-to-net\ CF \quad (13)$$

The estimated gross-to-net conversion factor is the ratio of the electrical energy delivered to grid to the gross output. SAM calculates this factor. The estimated net capacity was 45MWe, taking the estimated gross-to-net conversion factor as 0.9. It should be noted that the definition of the three terms is the same for all three CSP systems in this project.

3.5.3 Solar Collector Assembly

A Solar Collector Assembly (SCA) is a component of the solar field that constitutes mirrors, receivers and support structures. In SAM, the characteristics of a SCA are defined. The collector geometry in SAM is defined in the user interface by imputing the reflective aperture area, aperture width, length of collector assembly and average surface-to-focus path length. According to research done by NREL, these are related by equation (14).

$$F_{avg} = w\sqrt{\frac{\left(4a^2+\left(\frac{w}{2}\right)^2\right)^2}{a^2}}\,\frac{12a^2+\left(\frac{w}{2}\right)^2}{12w\left(4a^2+\left(\frac{w}{2}\right)^2\right)} \qquad (14)$$

In the formular a is the focal length and w the aperture width.

The SCA collector used in this analysis is the Siemens Sun Field 6 whose specs are given in the Table 4.

Table 4 SCA properties (SAM, 2020)

SCA Property	Value	Property	Value
SCA Length(m)	95.2	Geometric accuracy	0.968
SCA aperture(m)	5.776	Mirror reflectance	0.925
SCA Aperture reflective area	545	Mirror cleanliness factor avg.	0.97
Average focal length	2.17	Dust envelope avg.	0.98
Incidence angle modifier coef. F0	1	Concentrator Factor	1
Incidence angle modifier coef. F1	-0.0753	Solar field availability	0.99
Incidence angle modifier coef. F2	-0.03698	Tracking error	0.99

3.5.4 Receivers

The parameters that must be defined in SAM are the receiver type and receiver geometry. The geometry is best defined by the parameters defined below. These are defined according to NREL.

Absorber tube inner diameter (m): this is the diameter of the receiver absorber tube.

Glass envelope inner diameter (m): the inner diameter of the receiver glass envelope tube, the surface exposed to the annular vacuum.

Glass envelope outer diameter (m): Outer diameter of the receiver glass envelope tube, the surface exposed to ambient air.

The receiver used in this analysis is the 2008 Schott PTR70Vaccum having a transmissivity of 0.963 and absorptivity 0.96 as indicated in SAM.

3.5.5 Solar Field

Key considerations for the solar field are given and defined by the following terms. The solar multiple plays a key role when sizing a parabolic trough solar system. The size of the solar field is heavily dependent on the solar multiple and as such the value chosen must be optimal. Increasing the solar field area increases the amount of solar energy tapped by the system and reduces the LCOE. However, having too large a solar field will produce more thermal energy that is required by the power block and auxiliary systems. Optimisation of solar multiple was done and 2.4 was chosen as the optimal number.

Solar Multiple (SM): This is the field aperture area expressed as a multiple of the aperture area required to operate the power cycle at its design capacity. The chosen solar multiple for PTR was 2.4. this was arrived at after optimisation of solar multiple considering LCOE (National Renewable Energy Laboratory, 2021b). The results of this optimisation are shown in Figure 33.

Field Aperture (m^2): this is total area on which solar energy is collected. This may differ slightly from the total mirror size.

Design point DNI (M/m^2): As defined earlier in previous chapters, the design point DNI is the DNI at the area being considered for project development. The design point DNI of 900W/m^2 was used to calculate the required aperture area to achieve the design capacity.

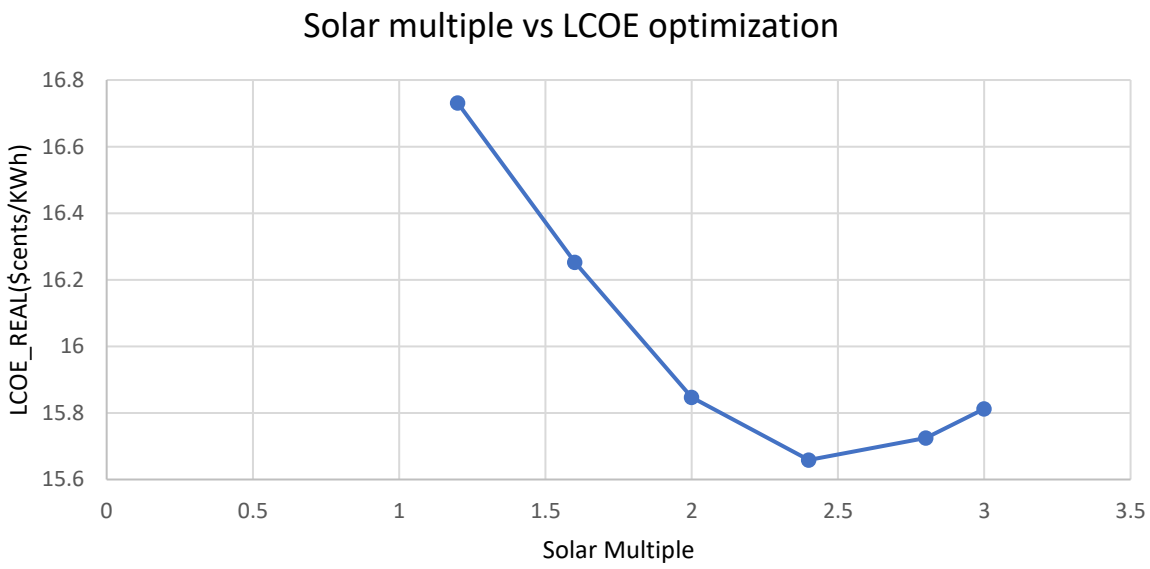

Figure 33 PTR solar multiple optimization

Field thermal power (MWt): this is the thermal power output expected from the solar receiver. It is related to the solar multiple and cycle thermal power by the equation given below.

$$field\ thermal\ power(MWt) = solar\ multiple\ x\ cycle\ thermal\ power(MWt) \quad (15)$$

Number of loops: this refers to the number of loops in the solar field. It is equal to the solar multiple multiplied by the number of loops required at a solar multiple of unity (1). This is always a whole number (National Renewable Energy Laboratory, 2021b).

Solar field efficiency

$$loop\ optical\ efficiency = SCA\ optical\ efficiency\ at\ design\ x\ HCE\ optical\ derate \quad (16)$$

The configuration of SCAs in a loop is shown in Figure 34. The number of SCA assemblies in a single loop was 12.

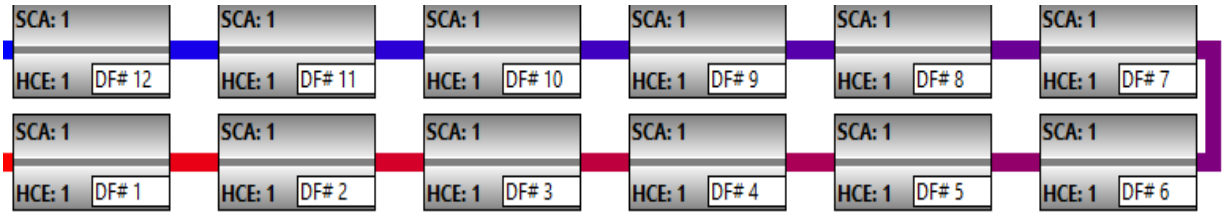

Figure 34 Loop configuration

3.5.6 Thermal Energy Storage

TES Thermal capacity (MWht). SAM computes the total heat transfer fluid volume in storage based on the storage hours at full load and the power block design turbine thermal input capacity (National Renewable Energy Laboratory, 2021b). The thermal storage capacity C is given by.

$$C = \frac{\dot{W}_{des\_gross}}{n\_des}\ x\ t_{full\_load} \quad (17)$$

$\dot{W}_{des\_gross}$ is the flow rate of the HTF in the collector, t_{full_load} is the total number of full load hours of thermal storage and n_des is the design thermal efficiency.

The estimated heat loss associated with the thermal storage system is estimated by the formula.

$$hl_{loss} = \left(h_{tank} * \pi * D_{tank} + \pi * \left(\frac{D_{tank}}{2}\right)^2\right) * N_{pairs} * (T_{TESave} - 20) * C_{hltank} \quad (18)$$

The full load hours for the PTR CSP were 10.

3.5.7 Heat Transfer Fluid

There are several options of HTF available for this system in SAM. Hitec solar salt will be used for the simulations in this project. This is particularly suitable for systems with TES because of its properties. It has minimum operating temperature of 238^{0}C, a maximum operating temperature of 593^{0}C and a specific heat capacity of 1.532KJ/Kg^{0}C (refer to

Appendix 11 for list of heat transfer fluids available in SAM). Summary of system parameters used in SAM for modelling PT system is given in Appendix 1.

3.6 Net Present Value

The Net Present Value was evaluated in SAM using the equation (18).

$$NPV = \sum_{i=0}^{P} \frac{C_i}{(1+d)^i} \tag{18}$$

In the equation, p is the period of analysis, i is number of years, C_i is the cashflow after tax and d is the discount rate.

The discount rate was calculated at 6.4% per annum for analysis period of 25 years. The NPV was calculated for all three CSP models. These figures reflect market trend values for CSP financial analysis according to recommendations by NREL. It should be noted that means of financing projects is not covered in this project. Basic financial inputs and results are what are considered.

LEFT INTENTIONALLY BLANK

4 Results and Discussion

SAM reports financial and performance model results for a year using 8760 hourly data points. Statistical summaries of data such as mean, maximum, total, standard deviation, average daily minimum and average daily maximum over the entire year or month for performance variables are also given in tabular, csv, or graphical format. For this project, only relevant performance and financial results were reported using tables and appropriate graphs. The summary results for parabolic trough, linear Fresnel and solar tower CSP are discussed below. The three systems were optimized to provide the highest rate of performance as described in chapter 3.

4.1 Parabolic Trough Collector CSP Results

Table 5 shows summary of results for the parabolic trough CSP model. The system simulated had a net power output of 45MW with 10 full load hours of TES (refer to appendix I for system specifications). The 132.24GWh of electricity produced annually accounts for close to 98% of the power consumed annually at the case study site. Furthermore, implementation of parabolic trough power plant would result in savings exceeding $7m annually. The negative NPV indicates that the payback period is longer than the analysis period and that the value of the energy savings is less than the cost of installing and running the project within the analysis period of 25 years. However, this should not worry the developer because this value entirely depends on the robustness involved in financing the project.

Table 5 Summary results for parabolic trough

Metric		Value
Performance	Annual Energy Produced	132,236,560KWh
	Capacity Factor	33.5%
	Annual water usage	32,068m^3
Financial	LCOE	5.85c/KWh
	Net Present Value	$-29,355,486
	Internal Rate of Return	Not achieved
	Net capital cost	$269,836,224
	Bill without system	$13,576,714
	Bill with system	$6,116,346
	Savings	$7,456,714

The LCOE for PT CSP was 5.85c/KWh. This compared competitively with the global LCOE average of 18.2c/KWh for CSP plants as of 2020 (Pitz-Paal *et al*., 2020). Comparison of the cost of this project to Andosol plant 50 MW PT CSP plant in Spain which has storage capacity of 7.5 hours and was estimated to cost $370m revealed that the direct cost investment was reasonable (Santos *et al*., 2018). However, total cost of developing the plant in Zambia may vary greatly due to factors such as location, labour and laws of the land.

Figure 35 shows a comparison of monthly energy produced against electricity load. In the months of May, June, July, August and September a total of 25.95GWh of electricity is exported to the grid. However, for months in which the system failed to meet the demand, a total of 28.39GWh is imported. The profile of generation is shown in Figure 36. The system is very active from about 9AM to 22PM. This production trend tallies with the weather profile for Zambia shown in Figure 23.

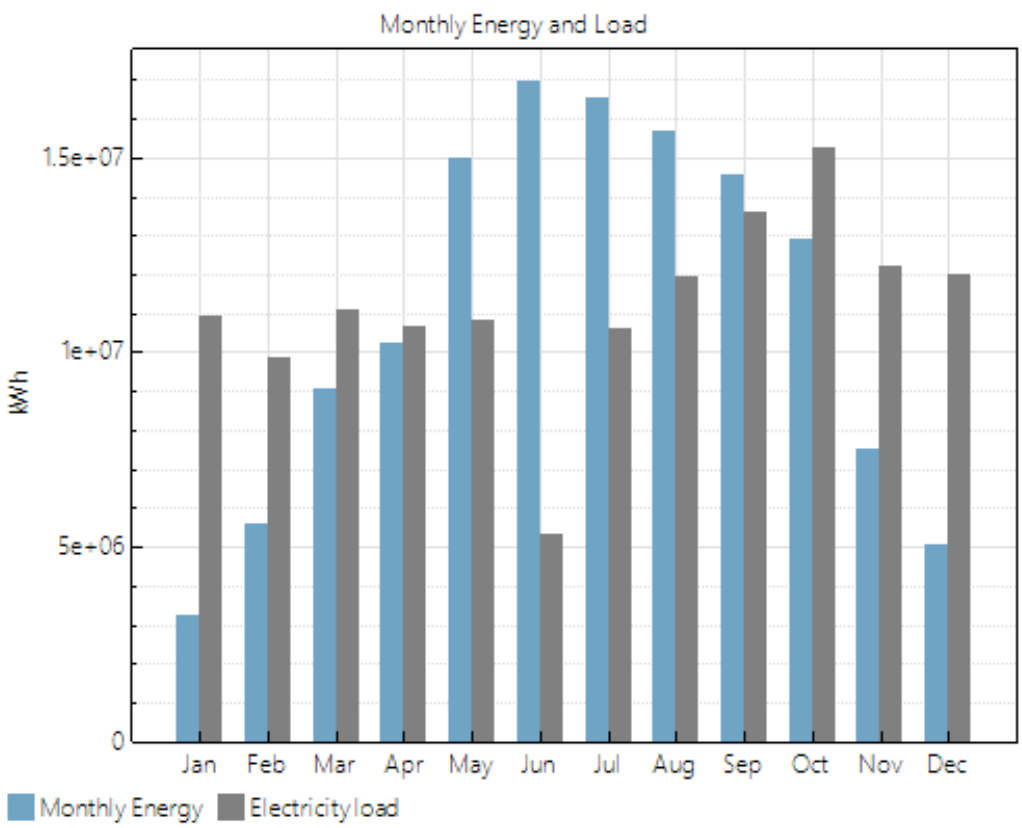

Figure 35 Monthly generation compared against load

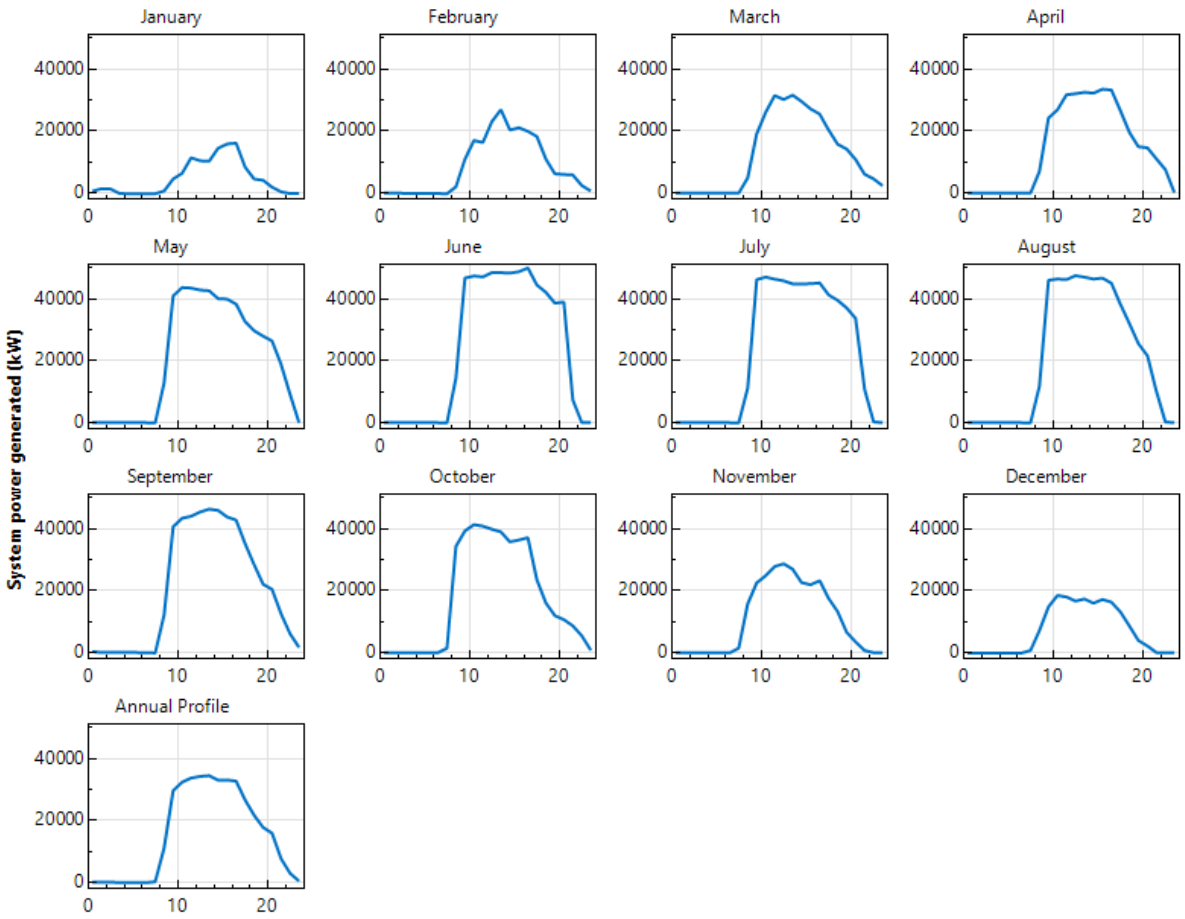

Figure 36 24hour profiles for PT system power generated for each month.

4.2 Linear Fresnel Receiver CSP results

Key financial and performance results for the LFR CSP model are shown in Table 6. The system simulated had 45MW net output with 10 full load hours of TES. The annual production from the optimized plant was 131.284GWh with a capacity factor of 33.3%. The plant used 12,032m^3 of water for cooling purposes annually. Ideally this water would be pumped from a nearby water stream. The results revealed that a LFR plant of 45MW net capacity would cut the annual energy cost by nearly 50%. The negative NPV indicated that the payback period is longer than the analysis period and that the value of the energy savings was less than the cost of installing and running the project within the analysis period of 25 years.

Table 6 Summary results for Linear Fresnel

Metric		Value
Performance	Annual Energy Produced	131,284,472KWh
	Capacity Factor	33.3%
	Annual water usage	12,032%
Financial	LCOE(Real)	9.72c/KWh
	Net Present Value	$-97,679,200
	Internal Rate of Return	Not achieved.
	Net Capital cost	$276,840,704
	Bill without system	$13,576,714
	Bill with system	$6,735,086
	Savings	$6,841,628

Close analysis of the results revealed that the annual energy produced from the plant would theoretically meet over 90% of the annual demand of the plant(134.3GWh). However, it is not practically feasible to achieve 90% because the optimal TES system can only operate for the 10hours at part load capacity. From Figure 38 one can notice that in May, June, July, august and September, the energy generated exceeded the load. The LCOE for LFR system was 6.31c/KWh which compares competitively with the global LCOE average of 18.2c/KWh as of 2020 (Pitz-Paal *et al*., 2020). Refer to appendix 5 for summary of costs.

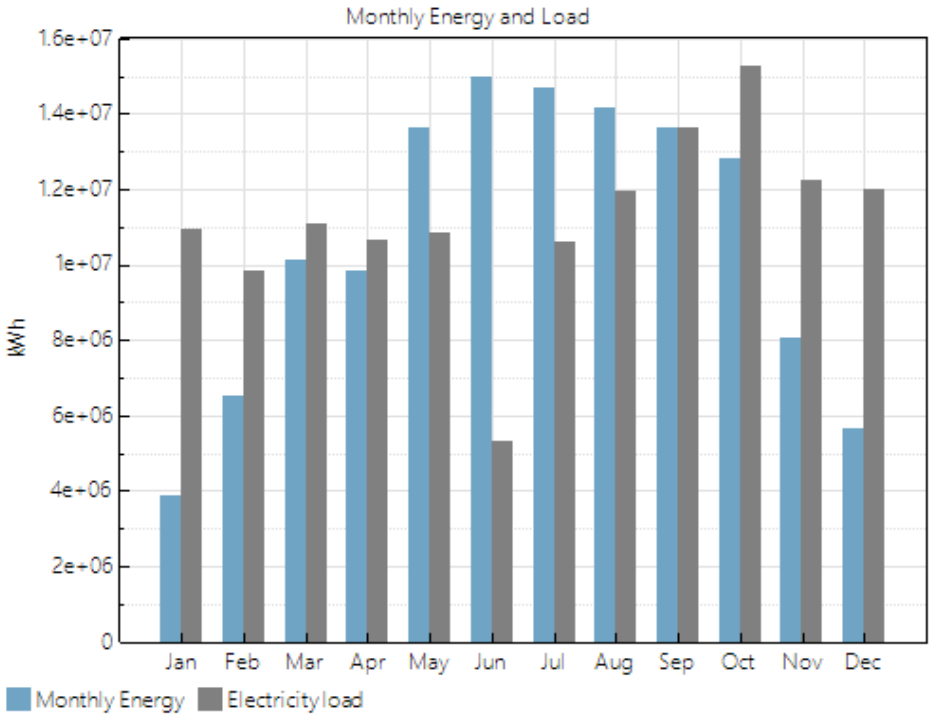

Figure 37 Monthly generation compared against load by LFR

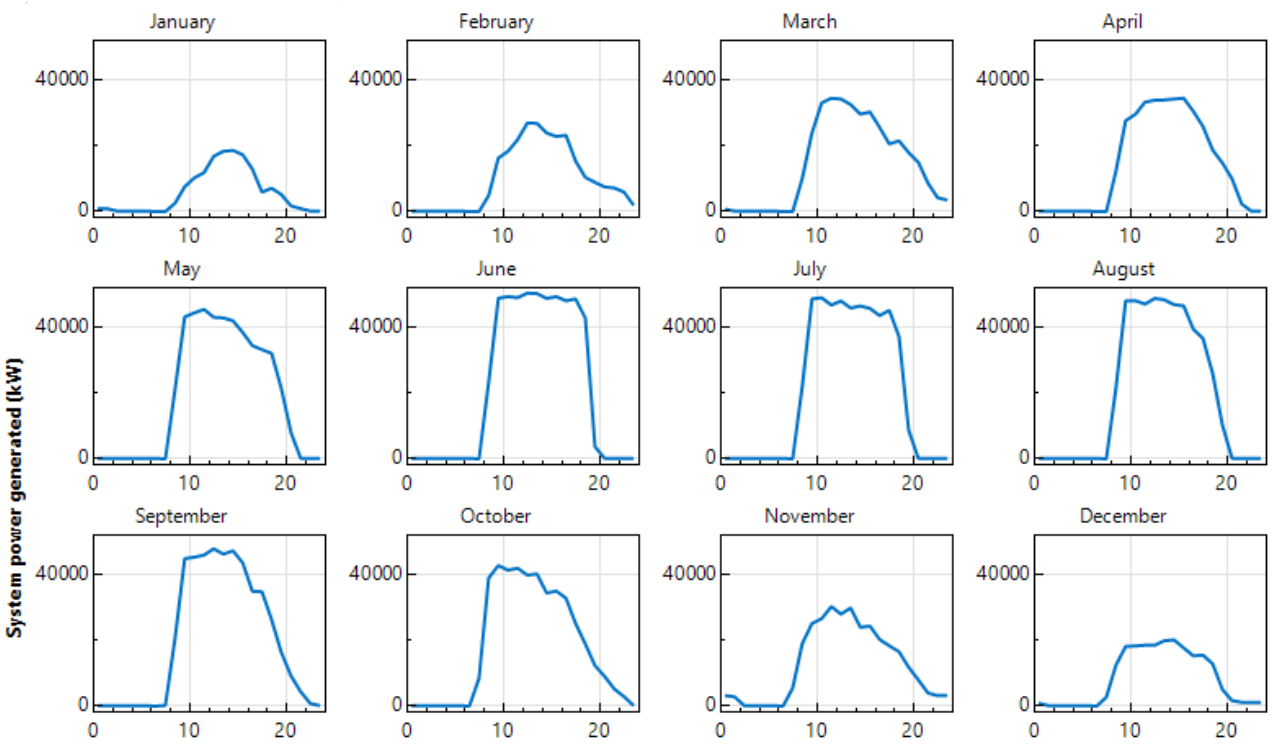

Figure 38 24 Hour profiles for LFR system power generated

Performance of the system improved in the months of June, through to October (refer to Figure 39). This production trend tallies with the weather profile for the case study site shown in Figure 23. In the months of May, June, July, August and September a total of 19.86GWh of electricity is exported to the grid. Nevertheless, for January, February, March, November and December the system did not meet the demand thus resulting in a total of 22.18GWh being imported. Production performance was lowest in January where only 3.9GW was generated. The highest production performance was observed in June where approximately 45MW was produced

4.3 Solar Tower CSP Results

Summary results for solar tower CSP model are shown in Table 7. The system simulated had a net power output of 45 MW with 12 full load hours of TES (refer to Appendix 3 for system specifications). Modelling a commercial ST CSP in SAM had no provision to input the load. Thus, analysis in relation to load was theoretically done in excel. The annual energy produced in this model was 174.976GWh with a capacity factor of 44.4%. The ST CSP model utilised more of its total installed capacity as compared to LFR (33.3%) and PT CSP (33.5%) models. The annual energy produced was 36.52GWh more than the annual load. The positive NPV showed that investment in the project was viable. The payback period was found to be 20 years at an Internal Rate of Return (IRR) of 11.0%. The analysis for this model was also 25 years.

Table 7 Summary results for solar tower

		Value
Performance	Annual Energy Produced	174,976,704KWh
	Capacity Factor	44.4%
	Annual Water Usage	36,840m^3
Financial	LCOE	13.42c/KWh
	Net Present Value	$22,862,990
	Internal Rate of Return	11.0% achieved in 20yrs
	Net capital cost	$350,074,528
	Bill without system	$13,676,724
	Bill with system	$1,036,700
	Savings	$12,640,024

LCOE reported in SAM for this model was 13.4c/KWh. The LCOE must be as low as reasonably possible because it sets a benchmark for the minimum economically viable price of electricity bought from the plant. The reported value was nearly 5-dollar cents less than the global average LCOE for concentrated solar power which stood at 18.2c/KWh as of 2020 (Pitz-Paal *et al*., 2020). The net cost of the system also compares favorably with recent market trends. A 50MW solar tower CSP plant developed in South

Africa costs about $9000/KWh on average (Noaman, 2014). The estimated total system cost per net capacity for this model was $10,826.54/KWh. It should be noted that costs are projected to become lower because of advancement in materials and manufacturing technologies.

SAM also provided a summary for the optimized recommended solar tower height, receiver-to-height ratio and receiver diameter. These were 124.235m, 12.5485 and 10.8052m, respectively. These were calculated through 48 iterations (see Appendix 5).

Profiles for energy generated revealed that the 45MW net CSP actively produced electricity for a significant portion of the year (see Figure 39). The months January and December had relatively low production this is the period which corresponds to rainy season in Zambia. The sky is predominately covered with nimbus clouds thus affecting the level of DNI. The average DNI in January is 100W/m^2, which is 4 times smaller than the DNI observed in June on average. This trend in performance is observed across all three systems simulated.

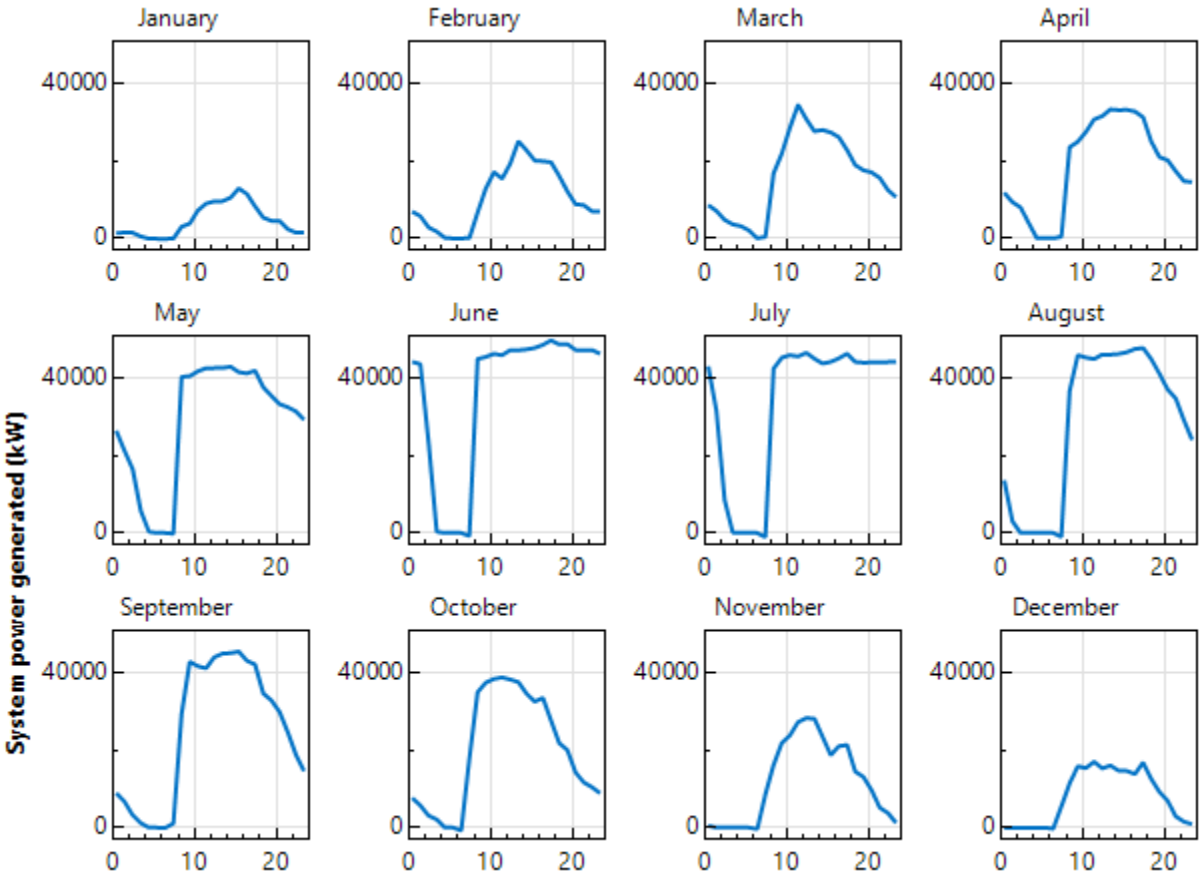

Figure 39 profiles for ST CSP system power generated.

Figure 40 shows a comparison of monthly energy produced against electricity load. From March to the beginning of October the net energy produced exceeded the load. The excess in this period was 61.91GWh while the deficit in the other months was 21.19GWh. The excess energy produced is almost three times the excess in LFR CSP model and over twice that in PT CSP model.

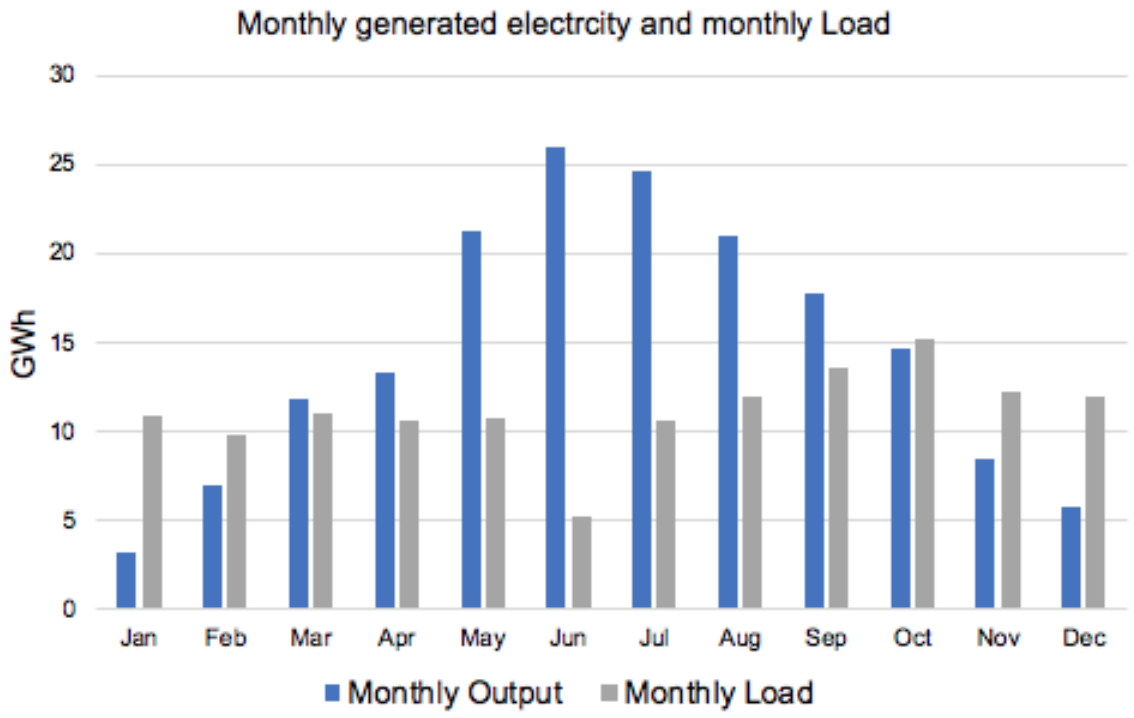

Figure 40 Monthly energy produced compared to electricity load.

4.4 Results validation

Output results from SAM were validated by reproducing performance results for an existing CSP system. The real life CSP system that was modelled is the Andasol-3 parabolic trough 50MW CSP plant in Aldeire Granada, Spain (Coordinates 37.22169, -3.06585). Dinter (2014) gives key specifications of Andasol 3 CSP. Summary of some key system inputs is given in Table 8.

The results shown in Table 9 revealed that SAM was able to reproduce the results with a relatively good accuracy. The annual output from the model was 4.4% lower than the actual design output at Andasol 3 CSP. The land area requirement predicted by the software was also off by 4.9%. This difference could have originated from the difference in layout between the actual plant and the model. It was not possible to model the plant with its exact specifications as most of the specifications could not be reproduced or found.

Table 8 Summary of key system specification for Andasol 3 and model

Specification	Andasol 3	SAM Model
Estimated net output (Nameplate)	49.9MW	49.9MW
Cycle thermal power	-	154
Solar Multiple	-	2
Solar field aperture area (m^2)	510,120	510,120
Solar field inlet temp(^oC)	293	293
Solar field outlet temp(^oC)	393	393
Receiver type	SKAL-ET 150	Schott PTR80
TES (Hours)	7.5	7.5
HFT	Thermal Oil	Therminol VP
Power Cycle	Rankine Cycle	Rankine Cycle

Table 9 Comparison of model results to actual existing system

Output parameter	Andasol 3 (49.9MW)	Model (50MW)	Difference
Annual Net Output (GWh)	165(Design)	157.767	-4.4%
Land Area(hectares)	200	209	+4.9%
Capital Cost	$370m	$309m	-16.4%
Capacity factor	37.7%	36.4%	-3.4%

The biggest difference was noticed in the cost of the model and the system. Andasol 3 was commissioned in 2011. The lower price of the model could be due to technical advancements in material and manufacturing technology that have occurred in the last decade. Nonetheless the results of model agree with that of the actual system with an acceptable level of accuracy to warranty validation. Further validation was done through sensitivity analysis.

4.4.2 Sensitivity Analysis

Sensitivity analysis was done in order to determine how variation in cost of key features of a parabolic trough plant model may have affected net capital cost. The main features known to affect capital cost are solar field, TES, land, HTF system and power block. The values used are consistent with values used by NREL in SAM.

Table 10 Parameters known to affect capital cost

Cost component	Mean cost	Standard Dev.
Solar field	$\$150/m^2$	22.5
Power block	$910/KWe	136.5
Land	$10000/acre	1500
HTF system	$\$60/m^2$	9

The tornado chat in Figure 41 revealed that land cost has the least effect on the net capital cost. However, variation in solar field size, power plant capacity and type of HTF employed affect the cost significantly. Thus, the discrepancy observed between the model and the actual system may have been as a result of a difference in the key parameters indicated on the tornado chat. This analysis strongly suggests that SAM produces reliable results. (Maronga, 2020 pp. 113-114) revealed similar findings in his thesis.

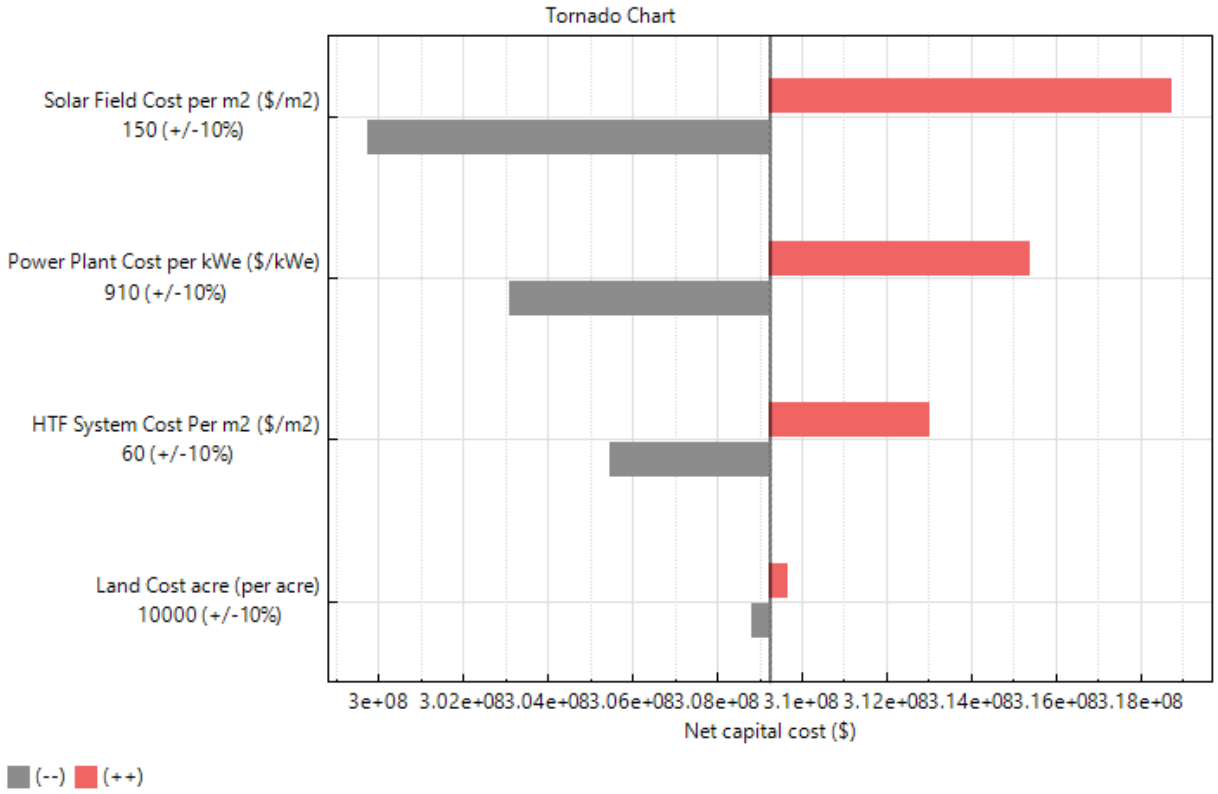

Figure 41 Cost analysis tornado chat

5 Conclusion

A quick comparison of the three systems revealed that solar tower CSP system was the most viable option for the site. Provided that climate conditions are suitable, the choice of CSP system depends largely on predications by software packages such as SAM which give predicted key performance indicators of plant performance such as predicated annual power output, capacity factor and Levelized Cost of Electricity (LCOE).

In this project, Solar tower CSP had the highest output of 174.98GWh. Results indicated that solar tower produced 32.6% more electricity than parabolic trough and 33.4% more than linear Fresnel CSP. Furthermore, solar tower CSP had the highest capacity factor of 44.4% which implied that it made use of 44.4% of its rated available output capacity for the analysis year resulting in savings in excess of $12.64M annually. The LCOE of the solar tower CSP was higher than that of the LFR and PT systems. Non the less, the reported value was nearly 5 cents lower than the global average LCOE for concentrated solar power which stood at 18.2 cents/KWh as of 2020 (Pitz-Paal *et al*., 2020).

The aim of this project was to model and assess the feasibility of powering a copper smelter plant with energy produced by CSP power plant. This objective was successfully achieved. A 50MW (gross) solar tower CSP system was found to be the most viable option. The net capital cost of this would be $350.074M. At an internal rate of return of 11.0% the investment would be recovered after 20years of operation. The development of a CSP plant at the case study site was found to be practically and financially feasible.

6 Further works

The Mining industry in Zambia accounts for nearly 50% of the total electrical energy consumed in the country. Thus, providing sustainable and clean energy for the mines will play a significant role in ensuring access to clean and affordable energy for the population. Further works proposed after this project include further research into how much land resource would be required to host CSP projects that could help to power the entire mining sector that consumes nearly 12TWh annually. CSP plants require huge areas of land to set up. Identification of potential sites that can host CSP projects within mining towns could be important for future consideration. A 50MW parabolic trough CSP plant like the Andasol-3 described in chapter 4.4, would require 200 Hectares of land.

Furthermore, Heliogen, a Bill Gates backed clean energy startup has taken the lead in research into green mining and smelting technology. One of their projects at Rio Tinto mine in the Mojave Desert will use concentrated solar energy to create extreme heat having temperatures in excess of a 1000^{o}C. This heat will be used to replace fossil fuel use in some of the heat intensive processes involved in mining (Egan, 2021).

Potential applications of CSP technology in the mining industry would be the replacement of high and low temperature processes. Among the possible applications include the production of SolarGas which could be used in place of natural gas as a fuel in the reduction process in the anode furnace in copper processing. SolarGas is natural gas that has been reformed by utilizing concentrated solar technology to produce carbon monoxide and hydrogen (Eglinton *et al.*, 2013). With such advancements in CSP technology application, mining companies in Zambia could engage in similar research too that would investigate potential application of concentrated solar technology in the key mining processes that require high and low heat applications.

References

Agyekum, E. B. and Velkin, V. I. (2020) 'Optimization and techno-economic assessment of concentrated solar power (CSP) in South-Western Africa: A case study on Ghana', *Sustainable Energy Technologies and Assessments*, 40(May). doi: 10.1016/j.seta.2020.100763.

Alinta Energy (2014) 'Port Augusta Solar Thermal Generation Feasibility Study Stage 1 - Pre-feasibility Study', (July). Available at: https://arena.gov.au/assets/knowledge-bank/2263503A-POW-RPT-001-RevD-Options-Study-Report.pdf.

Barhorst, N. (2016) 'Green hydrogen', *39th World Energy Engineering Conference, WEEC 2016*, 2, pp. 886–897.

Bojek, B. (2020) *Concentrating Solar Power (CSP)*. Available at: https://www.iea.org/reports/concentrating-solar-power-csp.

Chen, R., Rao, Z. and Liao, S. (2018) 'Determination of key parameters for sizing the heliostat field and thermal energy storage in solar tower power plants', *Energy Conversion and Management*, 177(September), pp. 385–394. doi: 10.1016/j.enconman.2018.09.065.

Craig, T. O., Brent, A. C. and Dinter, F. (2017) 'Concentrated solar power (CSP) innovation analysis in South Africa', *South African Journal of Industrial Engineering*, 28(2), pp. 14–27. doi: 10.7166/28-2-1640.

Egan, M. (2021) 'Project Planet; This Bill Gates-Backed Startup will soon help power a giant mine', *CNN Business*, 24 March. Available at: https://edition.cnn.com/2021/03/24/business/heliogen-solar-bill-gates-rio-tinto/index.html?fbclid=IwAR2DkVf8F0aTXO3g00WuTNBE88Brt-rPPDGv7RbrkBoUp0-bvm5fKjFSINU (Accessed: 10 June 2021).

Eglinton, T. *et al.* (2013) 'Potential applications of concentrated solar thermal technologies in the Australian minerals processing and extractive metallurgical industry', *JOM*, 65(12), pp. 1710–1720. doi: 10.1007/s11837-013-0707-z.

Energy Regulation Board (2019) *Energy Sector Report 2019*, *Energy Sector Report*. Available at: https://erb.org.zm/reports/esr2019.pdf.

German Aerospace Center (no date) *Insitute of Solar Research*. Available at: https://www.dlr.de/sf/en/desktopdefault.aspx/tabid-11688/20442_read-44865/ (Accessed: 24 June 2021).

Heller, P. (2017) *Introduction to CSP Systems and Performance*, *The Performance of Concentrated Solar Power (CSP) Systems: Analysis, Measurement and Assessment*. Elsevier Ltd. doi: 10.1016/B978-0-08-100447-0.00001-8.

IEA (2021) 'Electricity Market Report – July 2021', (July), pp. 1–123. Available at: https://www.iea.org/reports/electricity-market-report-july-2021.

Igogo, T. *et al.* (2020) 'Integrating Clean Energy in Mining Operations : Opportunities ,

Challenges , and Enabling Approaches Integrating Clean Energy in Mining Operations : Opportunities , Challenges , and Enabling Approaches Kwame Awuah-Offei', (July). Available at: https://www.nrel.gov/docs/fy20osti/76156.pdf.

IRENA (2012) *Renewable Energy Technologies: Cost Analysis Series*. Available at: https://www.irena.org/-/media/Files/IRENA/Agency/Publication/2012/RE_Technologies_Cost_Analysis-CSP.pdf.

IRENA (2019) *Renewable Power Costs 2019*. doi: 978-92-9260-244-4.

IRENA (2020) *Innovation Outlook: Thermal Energy Storage*. Available at: https://www.irena.org/publications/2020/Nov/Innovation-outlook-Thermal-energy-storage.

Jorgenson, J. *et al.* (2013) 'Estimating the Performance and Economic Value of Multiple Concentrating Solar Power Technologies in a Production Cost Model. A Report by the National Renewable Energy Laboratory, United States.', *National Renewable Energy Laboratory*, (December), p. 37. Available at: http://www.nrel.gov/docs/fy14osti/58645.pdf.

Link, J. (2021) 'CSP for mines: baseload and storage a must for extractive industry', *Energy and Mines Australia*. Available at: https://energyandmines.com/2015/10/solar-solutions-for-mines-supply-qa-with-joel-link-solarreserve/ (Accessed: 15 June 2021).

Lovegrove, K. and Pye, J. (2012) *Fundamental principles of concentrating solar power systems*. 2nd edn, *Concentrating Solar Power Technology*. 2nd edn. Elsevier Ltd. doi: 10.1016/b978-0-12-819970-1.00013-x.

Maronga, A. (2020) *Modelling and Assessing CSP and PV systems technical and economic performances to supply power to a mining context in Zimbabwe*. University of Strathclyde. Available at: http://www.esru.strath.ac.uk/Documents/MSc_2020/Maronga.pdf.

Mining for Zamiba (2016) *Energy and the mining industry*. Available at: https://miningforzambia.com/energy-and-the-mining-industry/ (Accessed: 23 June 2021).

Mwanza, M. *et al.* (2017) 'Assessment of solar energy source distribution and potential in Zambia', *Periodicals of Engineering and Natural Sciences*, 5(2), pp. 103–116. doi: 10.21533/pen.v5i2.71.

National Renewable Energy Laboratory (2021a) *System Advisor Model*. Available at: https://sam.nrel.gov/ (Accessed: 24 June 2021).

National Renewable Energy Laboratory (2021b) 'System Advisor Model', *SAM Help Manual*. Available at: https://sam.nrel.gov.

Nelson, V. C. (2020) *Introduction to Renewable Energy*, *Introduction to Renewable Energy*. doi: 10.1201/9781439891209-12.

Ngoc, T. *et al.* (2013) *Handbook of Energy*. doi: 10.1016/B978-0-08-046405-3.00010-3.

Noaman, M. B. (2014) 'Solar Power Tower Plant in Egypt', (September). doi:

10.13140/RG.2.2.31466.36809.

Ong, S. *et al.* (2013) 'Land-Use Requirements for Solar Power Plants in the United States', *Nrel/Tp-6a20-56290*, (June), p. 47.

Pitz-Paal, R. (2020) 'Concentrating solar power', *Future Energy: Improved, Sustainable and Clean Options for Our Planet*, pp. 413–430. doi: 10.1016/B978-0-08-102886-5.00019-0.

Py, X., Azoumah, Y. and Olives, R. (2013) 'Concentrated solar power: Current technologies, major innovative issues and applicability to West African countries', *Renewable and Sustainable Energy Reviews*, 18, pp. 306–315. doi: 10.1016/j.rser.2012.10.030.

Santos, J. J. C. S. *et al.* (2018) 'Concentrating Solar Power', *Advances in Renewable Energies and Power Technologies*, 1(2), pp. 373–402. doi: 10.1016/B978-0-12-812959-3.00012-5.

SolarPACES (2020) *CSP projects around the world*. Available at: https://www.solarpaces.org/csp-technologies/csp-projects-around-the-world/ (Accessed: 27 May 2001).

Thermal Energy Systems Specialists (2019) *TRNSYS*. Available at: http://www.trnsys.com/ (Accessed: 24 June 2021).

Tsoutsos, T., Frantzeskaki, N. and Gekas, V. (2005) 'Environmental impacts from the solar energy technologies', *Energy Policy*, 33(3), pp. 289–296. doi: 10.1016/S0301-4215(03)00241-6.

United States Agency for International Development USAID (2020) *Zambia energy sector overview*. Available at: https://www.usaid.gov/powerafrica/zambia.

Zablocki, A. (2019) *Fact Sheet | Energy Storage*, *Environment and Energy Study Institute*. Available at: https://www.eesi.org/papers/view/energy-storage-2019 (Accessed: 10 July 2021).

Appendices

Appendix 1 Summary specifications for parabolic trough systems

Table 11 specifications for parabolic trough systems (Bishoyi and Sudhakar, 2017; National Renewable Energy Laboratory, 2021a)

Specification	Value	Specification	Value
Solar Collector Assemblies		**Power Cycle**	
model type	Euro Trough ET150	Design gross output	50MWe
Reflective aperture area	817.5m^2	Estimated gross to net conversion Factor	0.9
Aperture width	5.75m	Estimated net output at design(nameplate)	45MWe
Length of collector assembly	0.115 m	**Heat Collector Elements**	
Glass envelope outer Diameter	150	Model Type	Siemens UVAC
No. Loops per assembly	12	Absorber flow pattern	Tube flow
Tracking error	0.99	Absorber Material	216L
Optical error	0.99	Inner surface roughness	4.5e-05
Geometry effects	0.98	**Rankine cycle**	
Mirror reflectance	0.935	Boiler operating pressure	80Bar
Dirt on mirror	0.97	Turbine inlet pressure	Fixed
Solar field		Condenser type	Air-cooled
Row Spacing	15m	Ambient temp at design	32
Header pipe roughness	4.57e-05	ITD at design	16
HFT pump efficiency	0.85	Condenser pressure ratio	1.0028
Pumping thermal loss coefficient	0.45	HTF hot temp	574^{0}C
Wind stow speed	25m/s	HTF cold temp	290^{0}C
Tracking power	277,500W	Rated cycle efficiency	0.397
HTF pump efficiency	0.85	**Thermal storage**	
HTF	Hitec Solar Salt	Full load hour of TES	10

Appendix 2 Summary of specifications for linear Fresnel system

Table 12 specifications for linear Fresnel system (Bishoyi and Sudhakar, 2017; National Renewable Energy Laboratory, 2021a)

Specification	Value	Specification	Value
Collector and Receiver		**Power Cycle**	
Type	Evacuated glass tube	Design gross output	50MWe
Relative aperture area	470.2m^2	Estimated gross to net conversion Factor	0.9
Collector module length	44.3m	Estimated net output at design(nameplate)	45MWe
Cross over piping length	15	**Rankine cycle**	
Piping distance between modules	1	Boiler operating pressure	100Bar
Collector azimuth angle	0^o	Turbine inlet pressure	Fixed
Tracking error derate	1	Condenser type	Air-cooled
Geometry effects derate	1	Ambient temp at design	32
Solar-weighted reflectivity	0.935	ITD at design	16
Dirt on mirror derate	0.95	Condenser pressure ratio	1.0028
General optical derate	0.732	HTF hot temp	574^{o}C
Solar field		Rated cycle efficiency	0.397
Solar multiple	2.5	**Thermal storage**	
Design DNI	850	Full load hour of TES	10
Design point wind speed	°c	HTF	Hitec solar salt
No. Collector modules in a loop	14		
No. of field sub sections	2		
Design loop inlet temp	294^{o}C		
Target outlet temp	525^{o}C		
Loop optical efficiency	0.61		

Appendix 3 Summary of specifications for solar power tower system

Table 13 specifications for solar power tower system (National Renewable Energy Laboratory, 2021a)

Specification	Value	Specification	Value
Heliostat field		**Power Cycle**	
Width	12.2m	Design gross output	50 MWe
Length	12,2m	Estimated gross to net conversion Factor	0.9
Ratio of reflective area to profile	0.97	Estimated net output at design(nameplate)	MWe
Single Heliostat Area	144.375m^2	**Rankine cycle parameters**	
Image error	1.53mRad	Boiler operating pressure	100Bar
Reflected image Conical error	4,32749mRad	Ambient temp at design	42°C
Deploy/stow angle	8Deg	ITD at design	16°C
Start-up energy	O.025kWe-hr	Cycle thermal efficiency	0.421
Wind stow speed	15m/s	Cycle thermal power	279.126MWt
Water usage	0.7L/m^3 63 washes per annum	HTF hot temp	574°C
Tower and Receiver		HTF cold temp	290°C
Tower height	To be determined by iteration	**Thermal Storage**	
Turndown fraction	0.25	Storage type	Two tanks
Maximum receiver operation fraction	1.2	TES capacity	2791.3MWt-hr
Receiver start-up delay	0.2hr	Available HTF volume	12,986m^3
Receiver start-up energy fraction	0.25	Tank height	12m
Coating absorbance	0.88	Storage tank volume	14166m^3
Coating emittance	0.94	Estimated heat loss	0.73
Heat loss factor	1(default)	Storage hours	12
Receiver HTF pump efficiency	0.85	Tank heater efficiency	0.99
HTF	Nitrate salt 60% NaNO3 40%KNO3	Cycle design HTF mass flowrate	652.4kg/s
		HTF cold and Hot temp	290°C, 574°C

Appendix 4 Parabolic trough CSP summary results.

Direct Capital Costs

Site improvements	430,336.0	m²	25.00 $/m2	$ 10,758,400.00
Solar field	430,336.0	m²	150.00 $/m2	$ 64,550,400.00
HTF system	430,336.0	m²	60.00 $/m2	$ 25,820,160.00
Storage	1,404.5	MWht	62.00 $/kWht	$ 87,078,648.00
Fossil backup	50.0	MWe, Gross	0.00 $/kWe	$ 0.00
Power plant	50.0	MWe, Gross	910.00 $/kWe	$ 45,500,000.00
Balance of plant	50.0	MWe, Gross	90.00 $/kWe	$ 4,500,000.00
			Subtotal	$ 238,207,616.00

Contingency

Contingency	7	% of subtotal	$ 16,674,533.00
		Total direct cost	$ 254,882,144.00

Figure 42 Direct capital costs

Metric	Value
Annual Net Electrical Energy Production	132,236,560 kWh-e
Annual Freeze Protection	450,509 kWh-e
Annual TES Freeze Protection	418,441 kWh-e
Annual Field Freeze Protection	32,068 kWh-e
Capacity factor	33.5%
Power cycle gross electrical output	151,153,344 kWh-e
First year kWh/kW	2,939 -
Gross-to-net conversion	87.5 %
Annual Water Usage	32,947 m^3
Levelized COE (nominal)	7.36 ¢/kWh
Levelized COE (real)	5.85 ¢/kWh
Electricity bill without system (year 1)	$13,576,060
Electricity bill with system (year 1)	$6,116,346
Net savings with system (year 1)	$7,459,714
Net present value	$-29,355,486
Simple payback period	NaN
Discounted payback period	NaN
Net capital cost	$296,836,224
Equity	$0
Debt	$296,836,224

Figure 43 Performance and financial metrics

Appendix 5 Solar tower summary results

Metric	Value
Annual energy (year 1)	174,976,704 kWh
Capacity factor (year 1)	44.4%
Annual Water Usage	36,840 m^3
PPA price (year 1)	14.48 ¢/kWh
PPA price escalation	1.00 %/year
Levelized PPA price (nominal)	18.23 ¢/kWh
Levelized PPA price (real)	14.48 ¢/kWh
Levelized COE (nominal)	16.90 ¢/kWh
Levelized COE (real)	13.42 ¢/kWh
Net present value	$22,862,990
Internal rate of return (IRR)	11.00 %
Year IRR is achieved	20
IRR at end of project	12.82 %
Net capital cost	$350,074,528
Equity	$153,595,264
Size of debt	$196,479,264

Figure 44 Summary of performance and financial data for solar tower

Direct Capital Costs

Heliostat Field						
Reflective area	1,269,054	m²	Site improvement cost	16.00	$/m²	$ 20,304,872.00
			Heliostat field cost	140.00	$/m²	
			Heliostat field cost fixed	0.00	$	$ 177,667,632.00
Tower						
Tower height	124.235	m				
Receiver height	12.5485	m	Tower cost fixed	3,000,000.00	$	
Heliostat height	12.2	m	Tower cost scaling exponent	0.0113		$ 12,188,572.00
Receiver						
Receiver area	1197.86	m²	Receiver reference cost	103,000,000.00	$	
			Receiver reference area	1571	m²	
			Receiver cost scaling exponent	0.7		$ 65,350,736.00
Thermal Energy Storage						
Storage capacity	2791.26	MWht	Thermal energy storage cost	22.00	$/kWht	$ 32,038,834.00
Power Cycle						
Cycle gross capacity	115	MWe	Fossil backup cost	0.00	$/kWe	$ 0.00
			Balance of plant cost	290.00	$/kWe	$ 14,500,000.00
			Power cycle cost	1,040.00	$/kWe	$ 52,000,000.00
					Subtotal	$ 374,050,656.00
Contingency						
			Contingency cost	7	% of subtotal	$ 26,183,546.00
					Total direct cost	$ 400,234,176.00

Figure 45 Set capital cost breakdown for solar tower

Finished with notices.

[31] 124.432 | 13.8739 | 9.16455 || 253.123 | 1039.61 | $1.33913e+08
[32] 124.048 | 13.4718 | 9.57836 || 252.691 | 1031.25 | $1.33974e+08
[33] 125.911 | 12.8761 | 10.0353 || 251.513 | 1034.23 | $1.33843e+08
[34] 128.189 | 12.7676 | 10.1733 || 251.279 | 1033.93 | $1.33896e+08
[35] 127.744 | 12.6317 | 10.4102 || 251.482 | 1022.69 | $1.34092e+08
[36] 130.334 | 12.6429 | 10.5294 || 251.774 | 1026.94 | $1.34441e+08
[37] 127.898 | 12.5369 | 10.3945 || 251.016 | 1029.58 | $1.33842e+08
[38] 125.814 | 12.5396 | 10.5787 || 252.02 | 1017.43 | $1.34407e+08
[39] 124.008 | 12.7669 | 10.4868 || 252.699 | 996.235 | $1.34549e+08
[40] 121.614 | 12.6389 | 10.0159 || 251.842 | 1031.41 | $1.33608e+08
[41] 129.178 | 12.9575 | 10.3034 || 252.254 | 1014.24 | $1.34625e+08
[42] 124.462 | 12.5761 | 10.6968 || 252.56 | 991.736 | $1.34634e+08
[43] 126.167 | 12.3858 | 10.8441 || 252.248 | 1008.86 | $1.34733e+08
[44] 124.146 | 12.5497 | 10.6731 || 252.459 | 994.868 | $1.34497e+08
[45] 121.648 | 12.4096 | 10.6019 || 252.704 | 990.464 | $1.34401e+08
[46] 126.15 | 12.7736 | 10.6164 || 252.933 | 1002.49 | $1.34984e+08
[47] 125.235 | 12.6466 | 10.6359 || 252.715 | 986.746 | $1.34638e+08
[48] 124.235 | 12.5485 | 10.8052 || 252.885 | 984.272 | $1.34822e+08

Algorithm converged:
tht= 124.235 rec_height= 12.5485 rec_diameter= 10.8052
Objective: 252.885

Save log OK

Figure 46 Summary results for solar tower

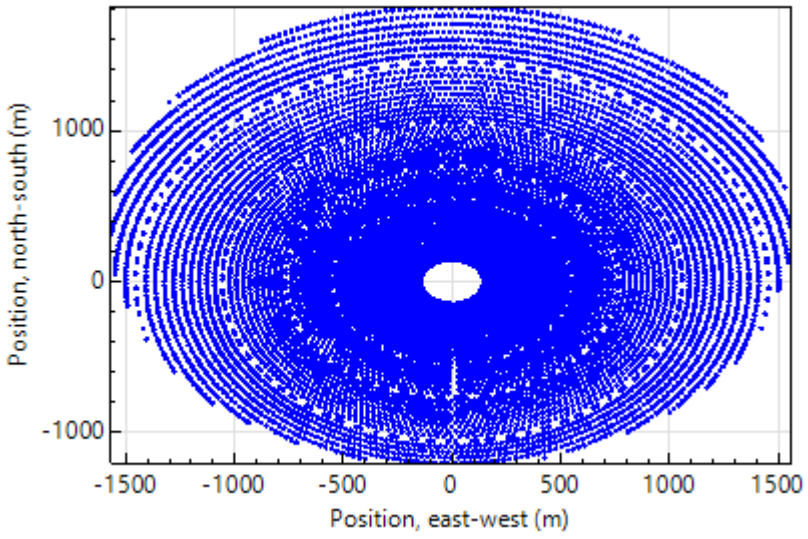

Figure 47 Optimized heliostat layout for ST CSP system

Appendix 6 Linear Fresnel summary results

Direct Capital Costs

Site improvements	511686	m²	20.00 $/m2	$ 10,233,728.00
Solar field	511686	m²	150.00 $/m2	$ 76,752,960.00
HTF system	511686	m²	47.00 $/m2	$ 24,049,260.00
Storage	1259.45	MWht	32.00 $/kWht	$ 40,302,268.00
Fossil backup	50	MWe, Gross	0.00 $/kWe	$ 0.00
Power plant	50	MWe, Gross	1,100.00 $/kWe	$ 55,000,000.00
Balance of plant	50	MWe, Gross	340.00 $/kWe	$ 17,000,000.00
			Contingency 7 %	$ 15,633,675.00
			Total direct cost	$ 238,971,888.00

Figure 48 Direct capital cost

Table 14 Performance and financial metrics for LFR

Metric	Value
Annual energy (year 1)	131,284,472 kWh
Capacity factor (year 1)	33.3%
Annual Water Usage	12,032 m^3
Levelized COE (nominal)	12.24 ¢/kWh
Levelized COE (real)	9.72 ¢/kWh
Electricity bill without system (year 1)	$13,004,029
Electricity bill with system (year 1)	$6,268,943
Net savings with system (year 1)	$6,735,086
Net present value	$-97,679,200
Simple payback period	NaN
Discounted payback period	NaN
Net capital cost	$276,840,704
Equity	$138,420,352
Debt	$138,420,352

Appendix 7 Dispatch schedule for all systems

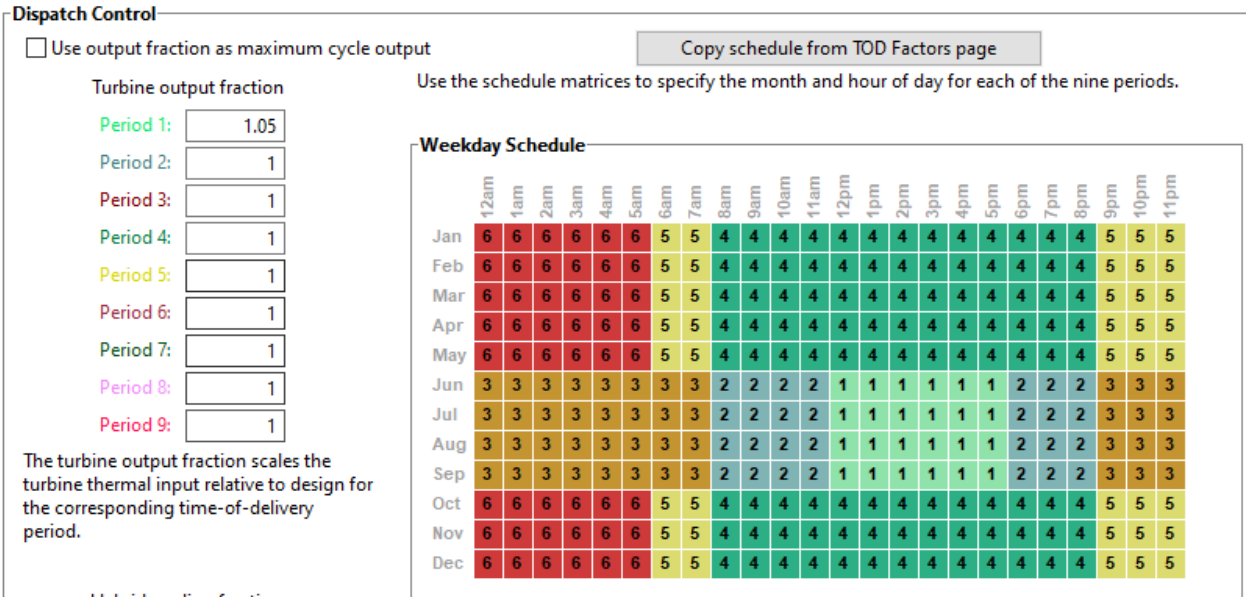

Figure 49 Dispatch schedule for all systems

Appendix 8 Heat maps

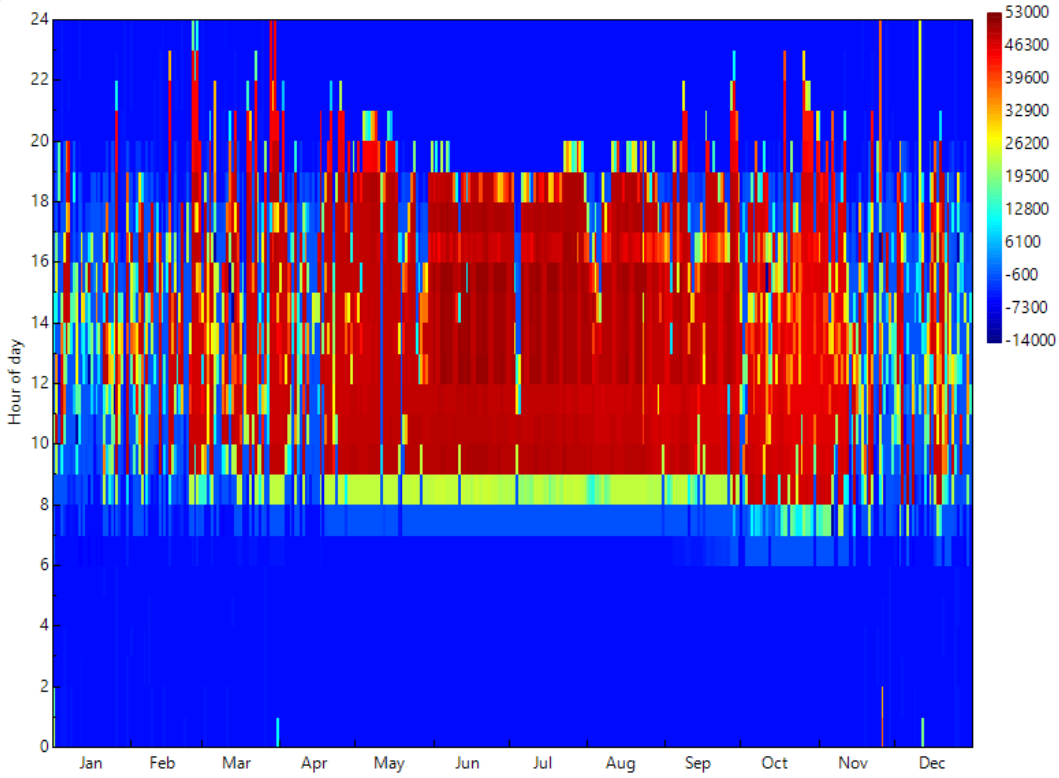

Figure 50 Hourly Electricity production for LFR CSP (KW)

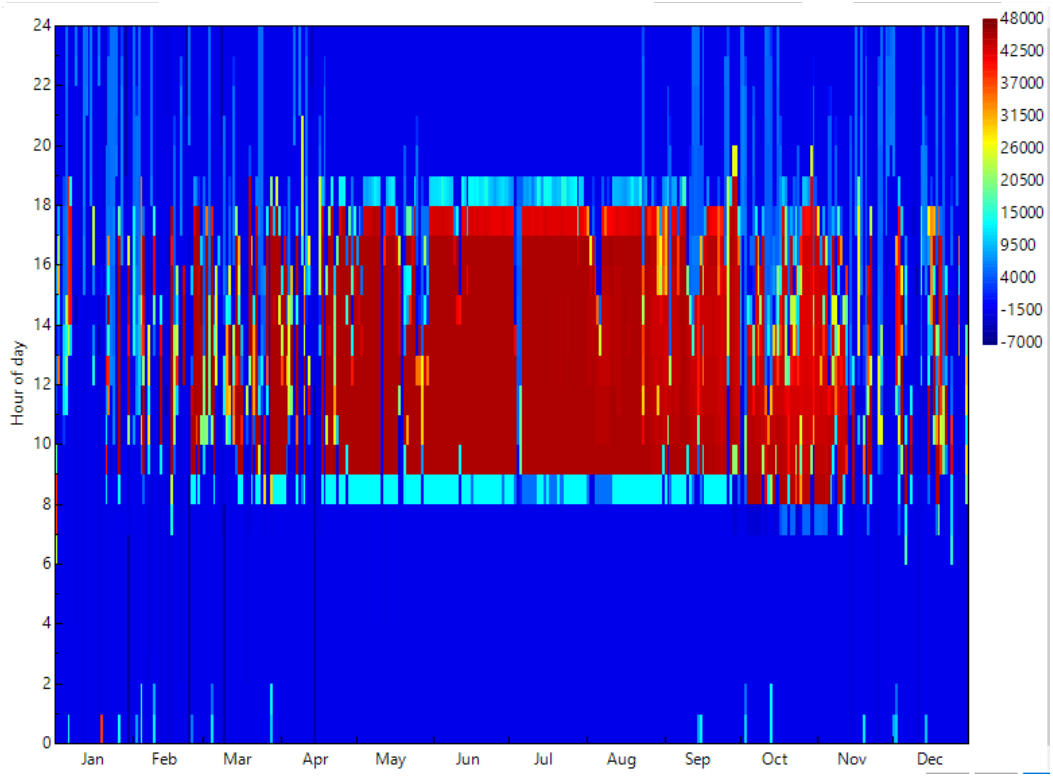

Figure 51 Electricity production for Parabolic trough (KW)

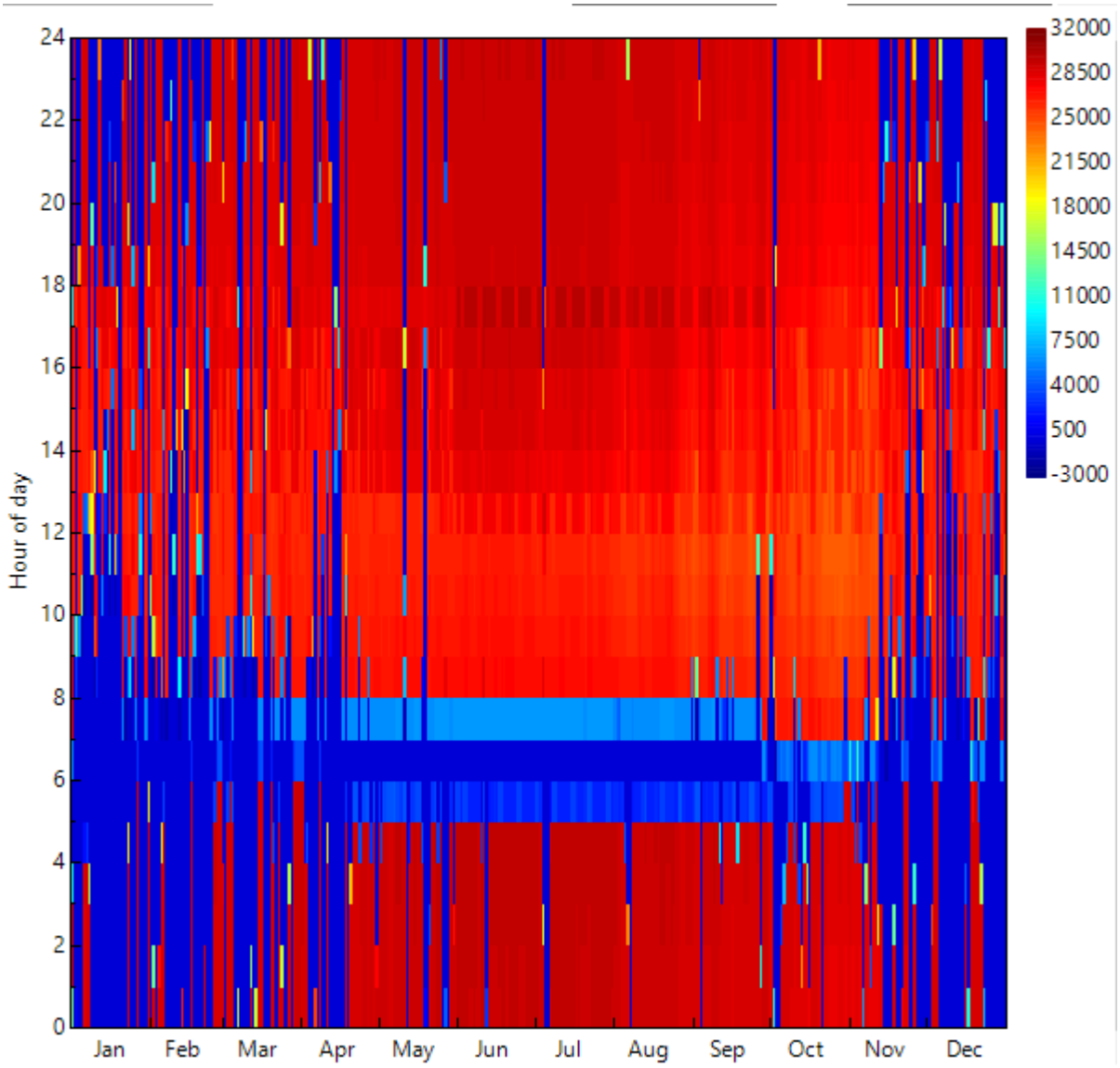

Figure 52 Electricity production for solar tower CSP

Appendix 9 Results for Andasol 3 CSP model

Metric	Value
Annual Net Electrical Energy Production	157,766,912 kWh-e
Annual Freeze Protection	1,994,888 kWh-e
Annual TES Freeze Protection	1,404,110 kWh-e
Annual Field Freeze Protection	590,779 kWh-e
Capacity factor	36.4%
Power cycle gross electrical output	180,005,104 kWh-e
First year kWh/kW	3,187 -
Gross-to-net conversion	87.6 %
Annual Water Usage	39,141 m^3
Levelized COE (nominal)	6.57 ¢/kWh
Levelized COE (real)	5.22 ¢/kWh
Electricity bill without system (year 1)	$360
Electricity bill with system (year 1)	$680,284
Net savings with system (year 1)	$-679,924
Net present value	$-107,395,520
Simple payback period	NaN
Discounted payback period	NaN
Net capital cost	$309,244,448
Equity	$0
Debt	$309,244,448

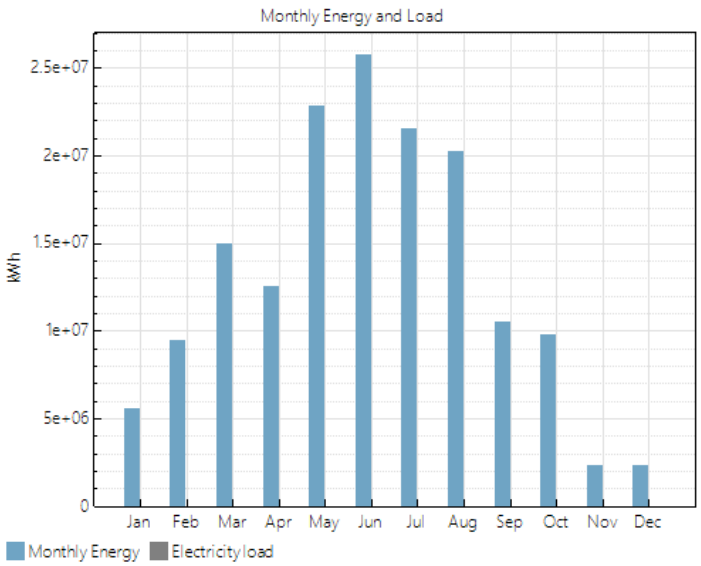

Figure 53 key performance metrics for Andasol 3 model

Direct Capital Costs

Site improvements	514,304.0	m²	25.00 $/m2	$ 12,857,600.00
Solar field	514,304.0	m²	150.00 $/m2	$ 77,145,600.00
HTF system	514,304.0	m²	60.00 $/m2	$ 30,858,240.00
Storage	1,158.7	MWht	62.00 $/kWht	$ 71,839,888.00
Fossil backup	55.0	MWe, Gross	0.00 $/kWe	$ 0.00
Power plant	55.0	MWe, Gross	910.00 $/kWe	$ 50,050,000.00
Balance of plant	55.0	MWe, Gross	90.00 $/kWe	$ 4,950,000.00
			Subtotal	$ 247,701,328.00

Contingency

Contingency	7	% of subtotal	$ 17,339,092.00
		Total direct cost	$ 265,040,416.00

Indirect Capital Costs

Total land area 445 acres Nameplate 50 MWe

	$/acre		% of direct cost		$/Wac		$		
EPC and owner cost	$ 0.00	+	11 %	+	$ 0.00	+	$ 0.00	=	$ 29,154,446.00
Total land cost	$ 10,000.00		0 %		$ 0.00		$ 0.00		$ 4,447,958.50

Sales Tax

Sales tax basis	80	Sales tax rate	5 %	$ 10,601,617.00
			Total indirect cost	$ 44,204,020.00

Total Installed Costs

Total installed cost excludes any financing costs from the Financial Parameters page.	**Total intalled cost** $ 309,244,448.00
	Estimated total installed cost per net capacity $ 6,247.36/kW

Figure 54 Capital cost for Andosol 3 model

Appendix 10 Differences of the four different CSP technologies

Table 15 Key differences of the four CSP technologies (adopted from (Santos et al., 2018, p10)

Characteristic	Parabolic Trough	Solar Tower	Linear Fresnel	Dish-Stirling
Typical capacity (MW)	10-300	10-200	10-200	0.01 -0.025
Maturity of technology	Commercial	Pilot/commercial projects	Pilot/Commercial projects	Demonstration projects
Technology development risk	Low	Medium	Medium	Medium
Operating temperature (°C)	350-550	250-565	390	550-750
Plant peak efficiency (%)	14-20	23-35*	18	30
Annual solar-to-electricity efficiency (net) (%)	01-Nov	01-Jul	13	01-Dec
Annual capacity factor (%)	25-28 (no TES) 29-43 (7h TES)	55 (10h TES)	22-24	25-28
Collector concentration	70-80 suns	>1 000 suns	>60 suns	>1 300 suns
Receiver/absorber	Absorber attached to collector, moves with collector, complex design	External surface or cavity receiver, fixed	Fixed absorber, no evacuation secondary reflector	Absorber attached to collector, moves with collector
Storage system	Indirect two-tank molten salt at 380 °C (ΔT=100K) or Direct two-tank molten salt at 550 °C (ΔT=300K)	Direct two-tank molten salt at 550oC (ΔT=300K)	Short-term pressurised steam storage (<10 min)	No storage for Stirling dish, chemical storage under development
Hybridisation	Yes, and direct	Yes	Yes, direct (steam boiler)	Not planned
Grid stability	Medium to high (TES or hybridisation)	High (large TES)	Medium (back-up firing possible)	Low
Cycle	Superheated Rankine steam cycle	Superheated Rankine steam cycle	Saturated Rankine steam cycle	Stirling
Steam conditions (°C/bar)	380 to 540/100	540/100 to 160	260/50	N/A
Maximum slope of solar field (%)	<1-2	<2-4	<4	10% or more
Water requirement (m^3/MWh)	3 (wet cooling) 0.3 (dry cooling)	2-3 (wet cooling) 0.25(dry cooling)	3 (wet cooling) 0.2(dry cooling)	0.05-0.1 (mirror washing)
Application type	On-grid	On-grid	On-grid	On-grid/Off-grid
Suitability for air cooling	Low to good	Good	Low	Best
storage with molten salt	Commercially available	Commercially available	Possible, but not proven	Possible, but not proven

Appendix 11 Heat transfer fluid for CSP application

Table 16 List of HTF fluids

Name	Type	Min Optimal Operating Temp °C	Max Optimal Operating Temp* °C	Freeze Point °C	Comments
Hitec Solar Salt	Nitrate Salt	238	593	238	
Hitec	Nitrate Salt	142	538	142	
Hitec XL	Nitrate Salt	120	500	120	
Caloria HT 43	Mineral Hydrocarbon	-12	315	-12 (pour point)	used in first Luz trough plant, SEGS I
Therminol VP-1	Mixture of Biphenyl and Diphenyl Oxide	12	400	12 (crystallization point)	Standard for current generation oil HTF systems
Therminol 59	Synthetic HTF	-45	315	-68 (pour point)	
Therminol 66	?	0	345	-25 (pour point)	
Dowtherm Q	Synthetic Oil	-35	330	n/a	
Dowtherm RP	Synthetic Oil	n/a	330	n/a	

END